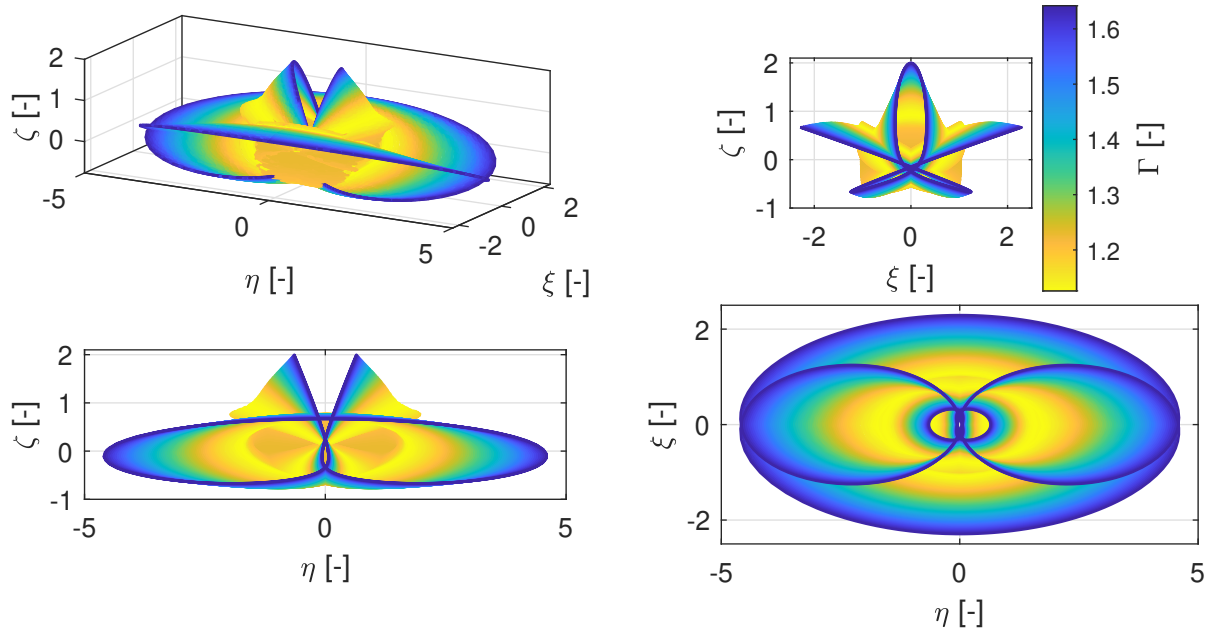

(a) Northern branch

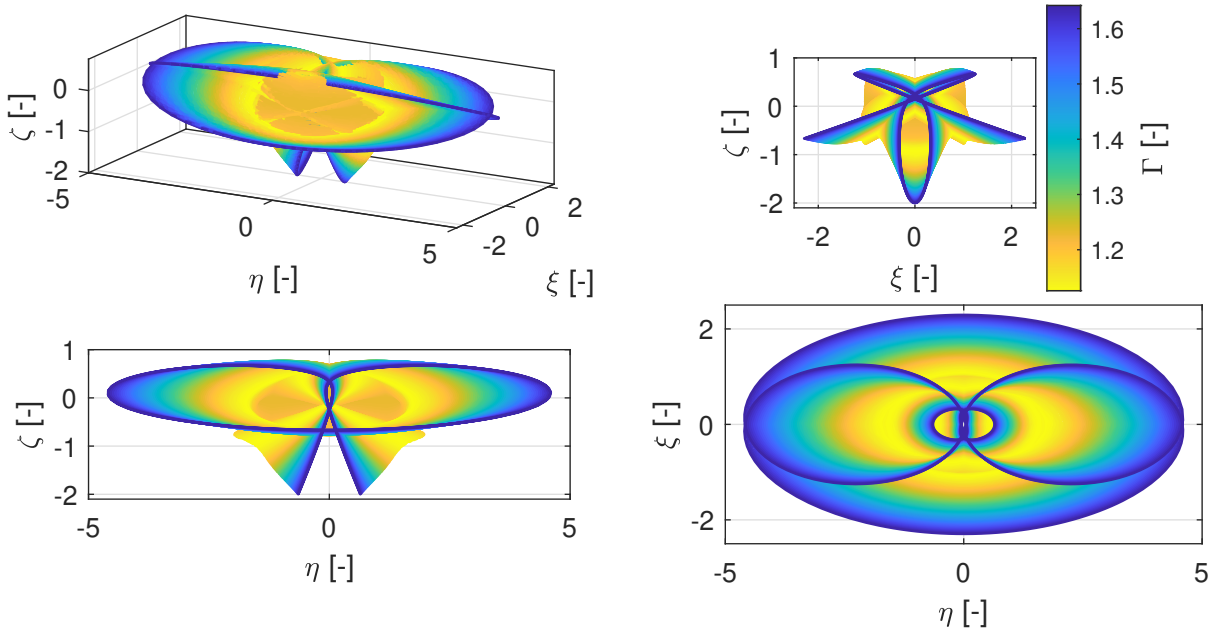

(b) Southern branch

Figure 5.28: Family evolution of the high-energy 3D-P5QSO$_1$ family in the H3BP

orbit is highly distorted, with two large inclined loops and a closer approach to the secondary compared to the others. The angular momentum projection is no longer a Jordan arc, as it now includes two additional side loops, illustrating the more complex behavior of this orbit.

The second family of this section is the 3D-P6QSO$_1$ family, depicted in Figures 5.29 and 5.30. Like with the previous family, each line of Figures 5.29a and 5.29b correspond to two different branches. However, this time it is because of the planar projection rather than the

z coordinate, as this family is z-symmetric. In this sense, the two perpendicular crossings to the x-z plane are located on different hemispheres for each orbit. As for the origin of the two branches, it is due to the single-symmetric nature of the planar projection, with and LSS branch (Figure 5.30a) and the RSS branch (Figure 5.30b). Another difference is that this time the stable part of the family that existed for the 3D-P5QSO$_1$ family does not exist for this one. In this sense, only the orbits right after the bifurcation possess a limited instability.

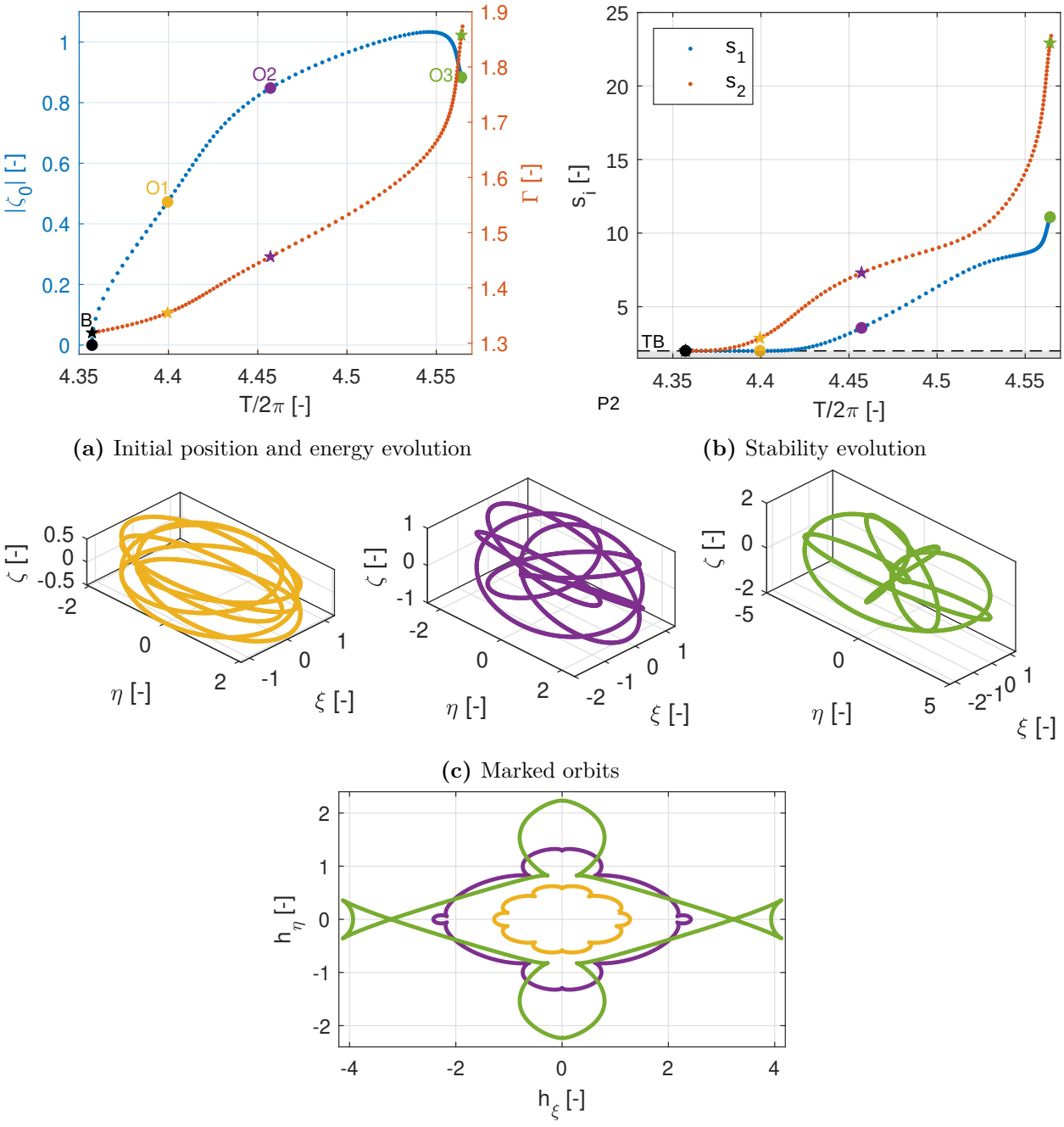

(a) Initial position and energy evolution

(b) Stability evolution

(c) Marked orbits

(d) Marked QSOs' rotating angular momentum

Figure 5.29: High-energy 3D-P6QSO$_1$ family in the H3BP

Finally, the three orbits selected for illustrating the evolution of the family showed a similar trend as the $m = 5$ family. The swing of the planar projection of the orbits increases from 'O1', which has more of a cylindrical shape, to 'O3', where this time there are 4 loops with a high inclination. Regarding the planar projection of the rotating angular momentum, this time is subdivided into 10 arcs, with one retrograde revolution for 'O1' and 'O2' and a self-intersecting line for 'O3', with the arcs completely distorted.

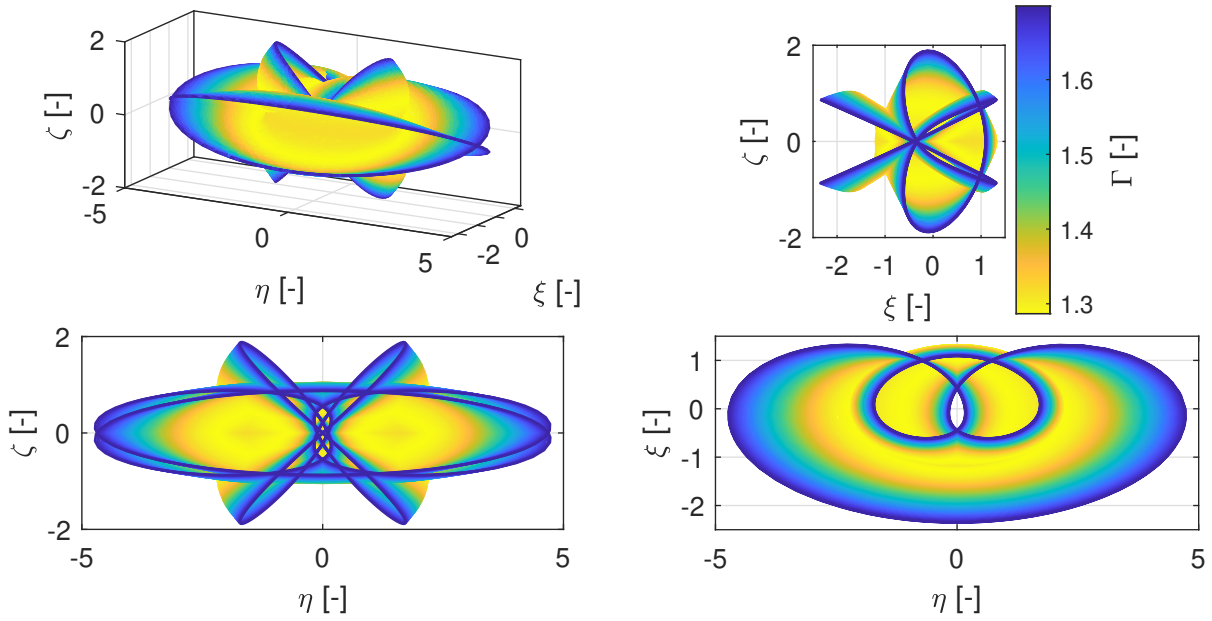

(a) LSS branch

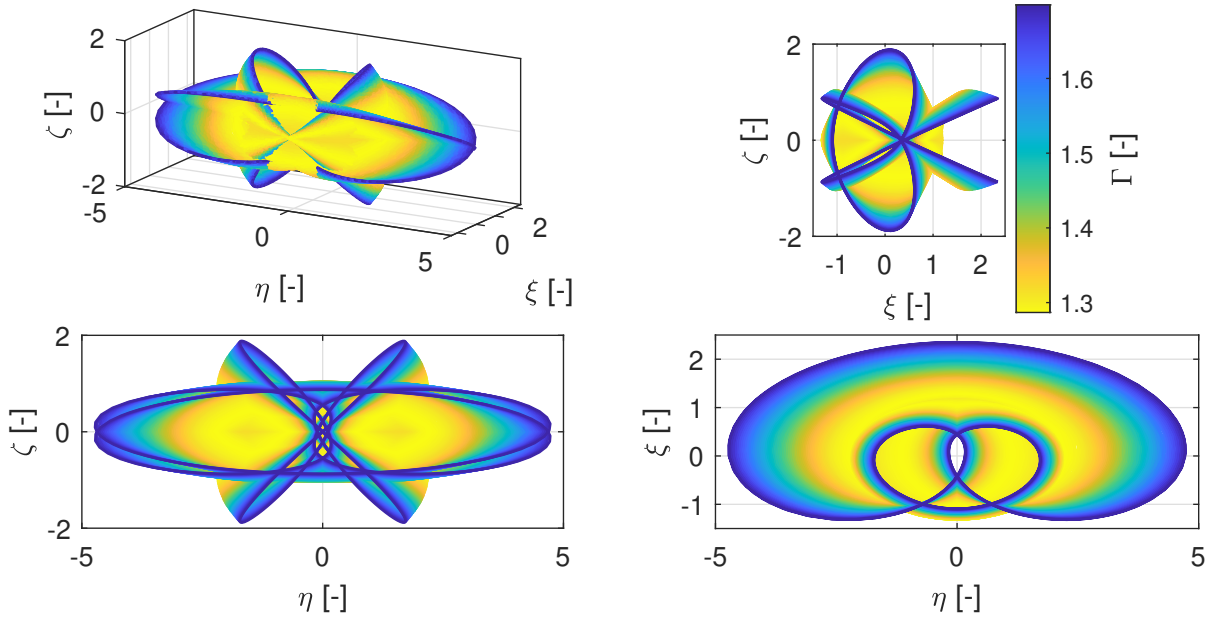

(b) RSS branch

Figure 5.30: Family evolution of the high-energy 3D-P6QSO$_1$ family in the H3BP

The final high-energy 3D family is the 3D-P7QSO$_1$, shown in Figures 5.31 and 5.32. Like

the family with multiplicity 5, it is composed of z-asymmetric DS QSOs. It has two branches: the northern one illustrated in Figure 5.32a and the southern one in Figure 5.32b. Another similarity is the presence of a region with stable or nearly stable suitable for long-term observations. Finally, the trend in orbital shape follows that of the two previous families. For the 'O1' orbit, this time, planar projection of the rotating angular momentum consists of 12 arcs, which are already highly distorted for the 'O2' orbit, though they still form a single retrograde loop.

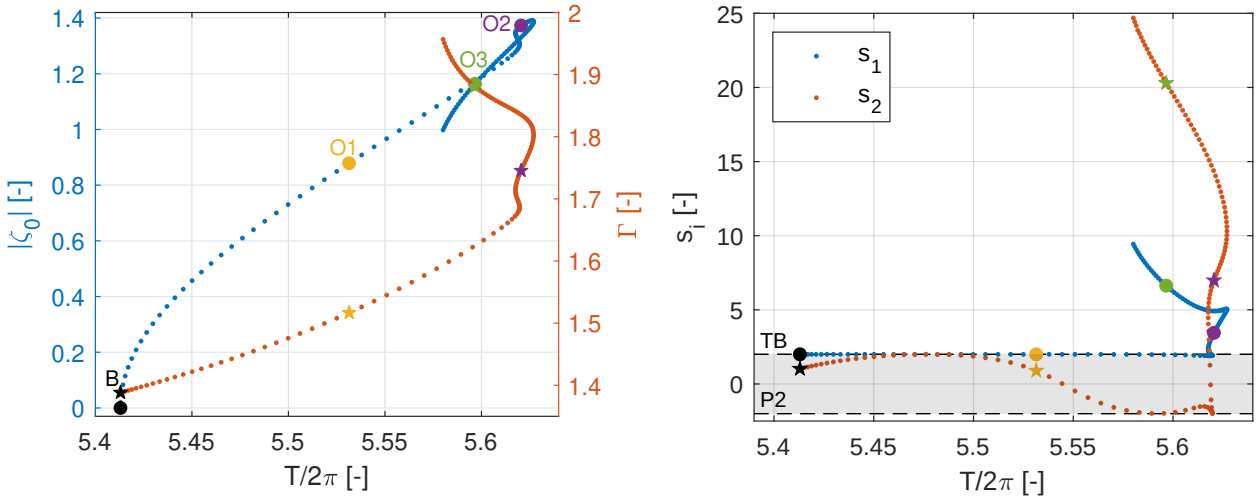

(a) Initial position and energy evolution

(b) Stability evolution

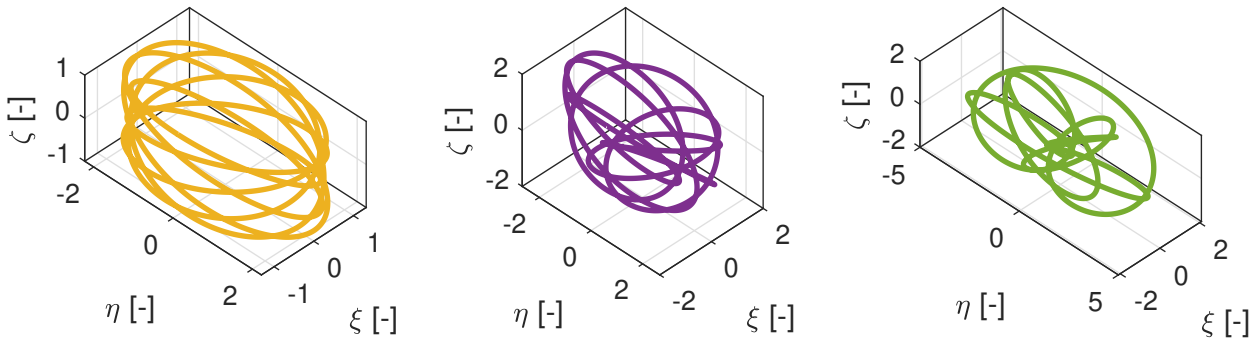

(c) Marked orbits

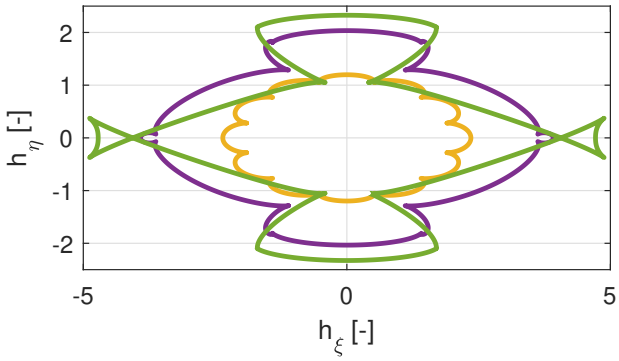

(d) Marked QSOs' rotating angular momentum

Figure 5.31: High-energy 3D-P7QSO$_1$ family in the H3BP

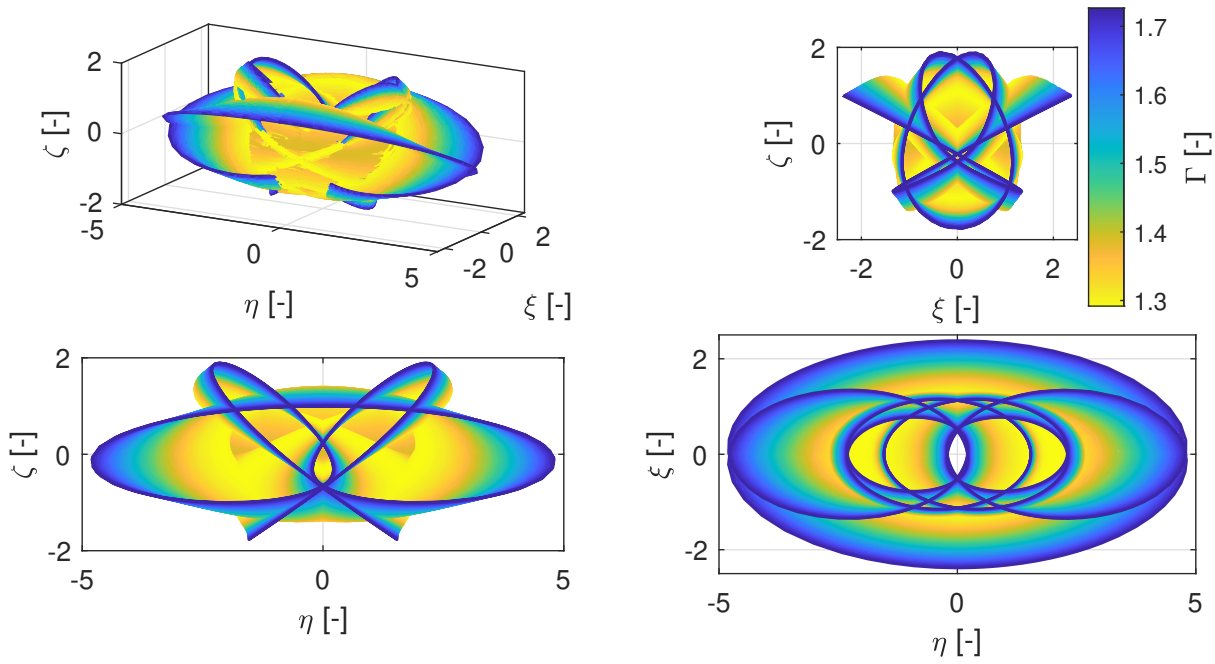

(a) Northern branch

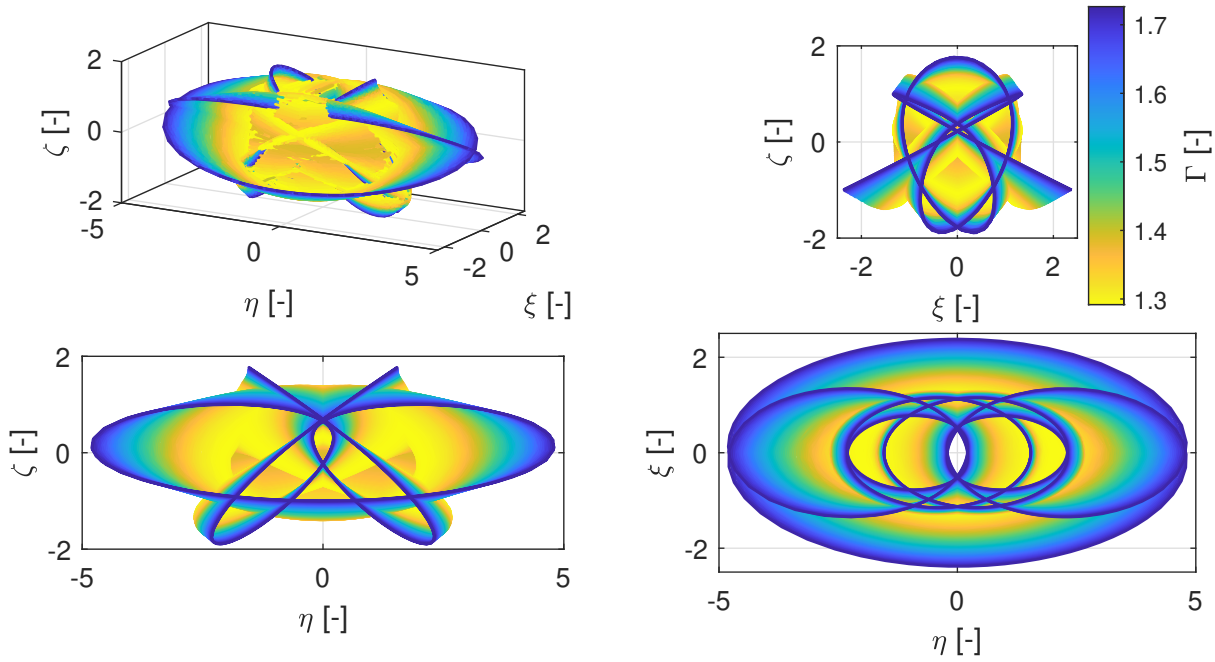

(b) Southern branch

Figure 5.32: Family evolution of the high-energy 3D-P7QSO$_1$ family in the H3BP

5.4.2 Low-energy Families

The first low-energy family is the 3D-P5QSO$_2$ and it is depicted in Figures 5.33 and 5.15. Like the high-energy family of multiplicity 5, the family is composed by two branches by z-asymmetric DS QSO, one with northern QSOs and the other with southern ones. Another

similarity with this family is that again some of the orbits of the family have a stable or near stable behavior. However, there are two characteristics of this family that differ from what has been seen yet.

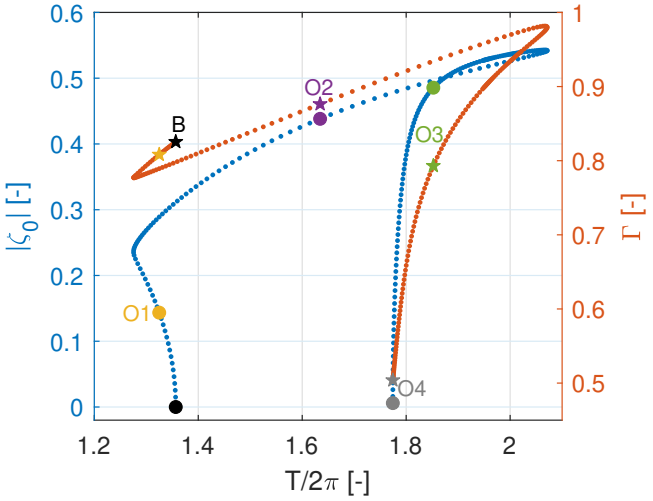

(a) Initial position and energy evolution

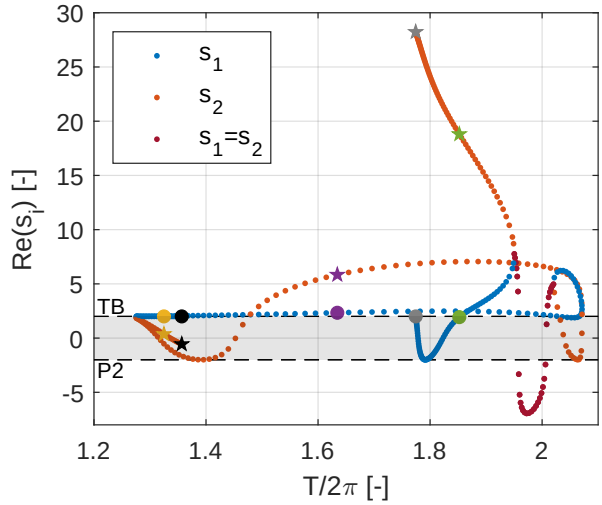

(b) Stability evolution

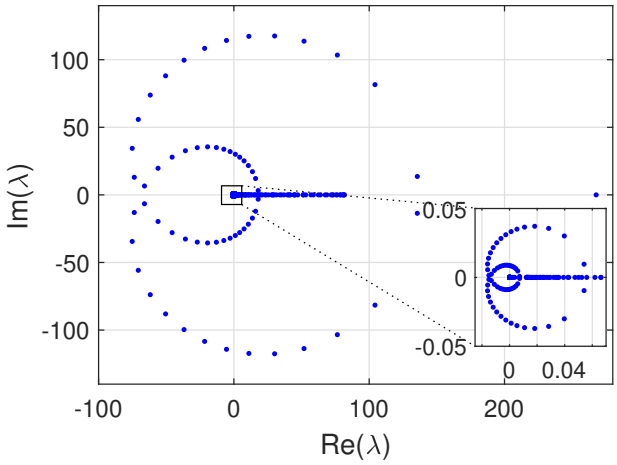

(c) $\mathcal{M}$ eigenvalues detail in the complex plane

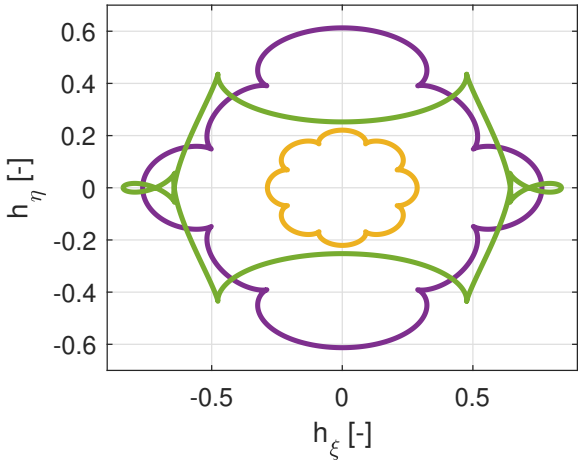

(d) Marked QSOs' rotating angular momentum

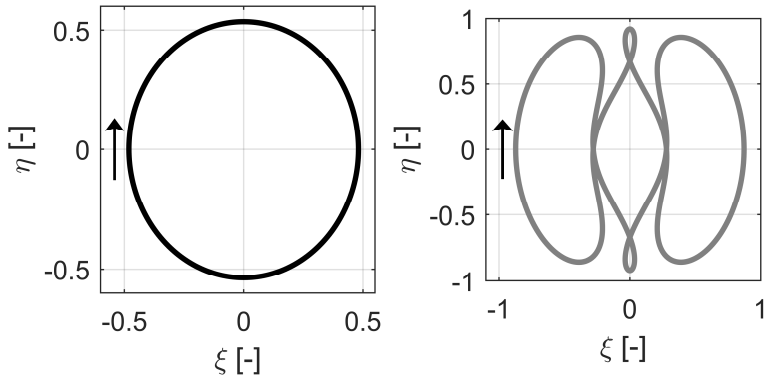

(e) Planar marked orbits

Figure 5.33: High-energy 3D-P5QSO$_2$ family in the H3BP

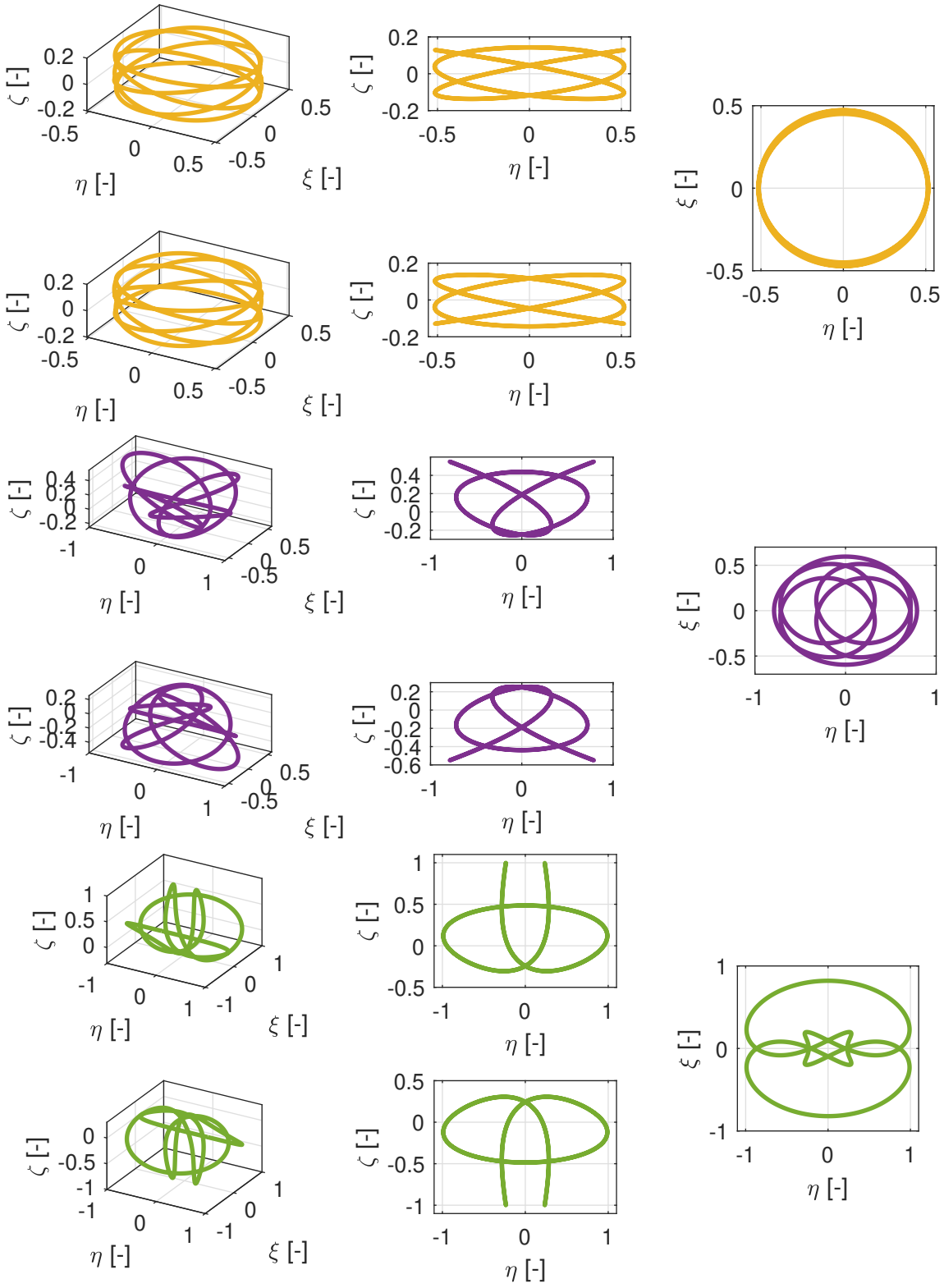

Figure 5.34: Marked 3D orbits of the high-energy 3D-P5QSO$_2$ family in the H3BP

The first one is that the family is bounded by two different planar orbits in which a bifurcation takes place and that are shown in Figure 5.33e. The first of them is the black 'B' orbit from which the 3D-family bifurcates from the steady QSO family through a period-quintupling bifurcation. The second of these orbits is the 'O4' gray one, that corresponds to a mixed orbit belonging to the already studied P3QSO family. This time the bifurcation that connects both families is a tangent bifurcation. The second special characteristic takes place at the stability indices and it is illustrated by the maroon color in Figure 5.33b. The part of the family represented by this color on the plot possesses the same value for the two stability indices. This situation is not out of coincidence, but corresponds to one of the situations of the eigenvalues explained in Section 4.2. This situation is detailed in Figure 5.33c, where it can be observed how the two pairs of eigenvalues are placed on the complex plane and out of the real axis. This situation can take place thanks to the coupling of the two none trivial pairs.

Finally, in Figure 5.34 the marked 3D QSOs are depicted and in 5.33d the projection of their angular momentum is shown. This time, to illustrate the two branches, in Figure 5.34, both the southern and northern versions of the marked orbits are represented, taking into account that the planar projection is common for both of them. The same evolution observed for previous families is maintained regarding the swing motion of the planar projection. Nonetheless, there is an important difference that is that this time the planar projection of the last orbit, the green 'O3', has a mixed behavior as part of the motion is retrograde and another part is prograde. As for the angular momentum, the behavior is the same one observed for the 3D-P5QSO$_1$ family, even though this time the shape for the 'O3' orbit is a bit different.

The second family is the 3D-P6QSO$_2$ one, depicted in Figures 5.35 and 5.36. Like the 3D-P6QSO$_1$ family, this family is composed by z-symmetric QSOs with a SS planar projection forming two branches, one of LSS QSOs and the other with RSS ones. Like the previous family, each branch is bounded by two planar orbits (Figure 5.35c). Again, the first of these orbits is a steady QSO propagated for six periods. The second one, represented in the figure by the 'O4' gray colored orbit, is a prograde orbit that belongs to the family of low prograde orbits (LPOs), which corresponds to the g' family in Hénon's work [25]. Contrary to the steady QSO in which a period-sixtupling bifurcation was found, the connection between the 3D-P6QSO$_2$ and the P3QSO families is through a period-quadrupling bifurcation. Regarding the stability index, this family has more bounded values, where a big part of the family is stable or almost stable.

Finally, the evolution of the family can be studied through the three marked orbits shown in Figure 5.36, where each orbit is shown for both branches the LSS and the RSS. This time, the vertical projection of each branch is common, whereas the planar projection of each branch is a mirror of the other with respect to the x-axis. Like with the previous families, right after the bifurcation from the steady QSO family, the orbits have an insignificant swing motion like the 'O1' yellow orbit. After that, the family has a phase in which all the loops of the orbits are vertical. At one point the motion stops to be completely retrograde and goes through a transition area with a mixed motion like 'O2'. Finally, the orbits become completely prograde and the swing motion reduces once again, as it can be observed in the

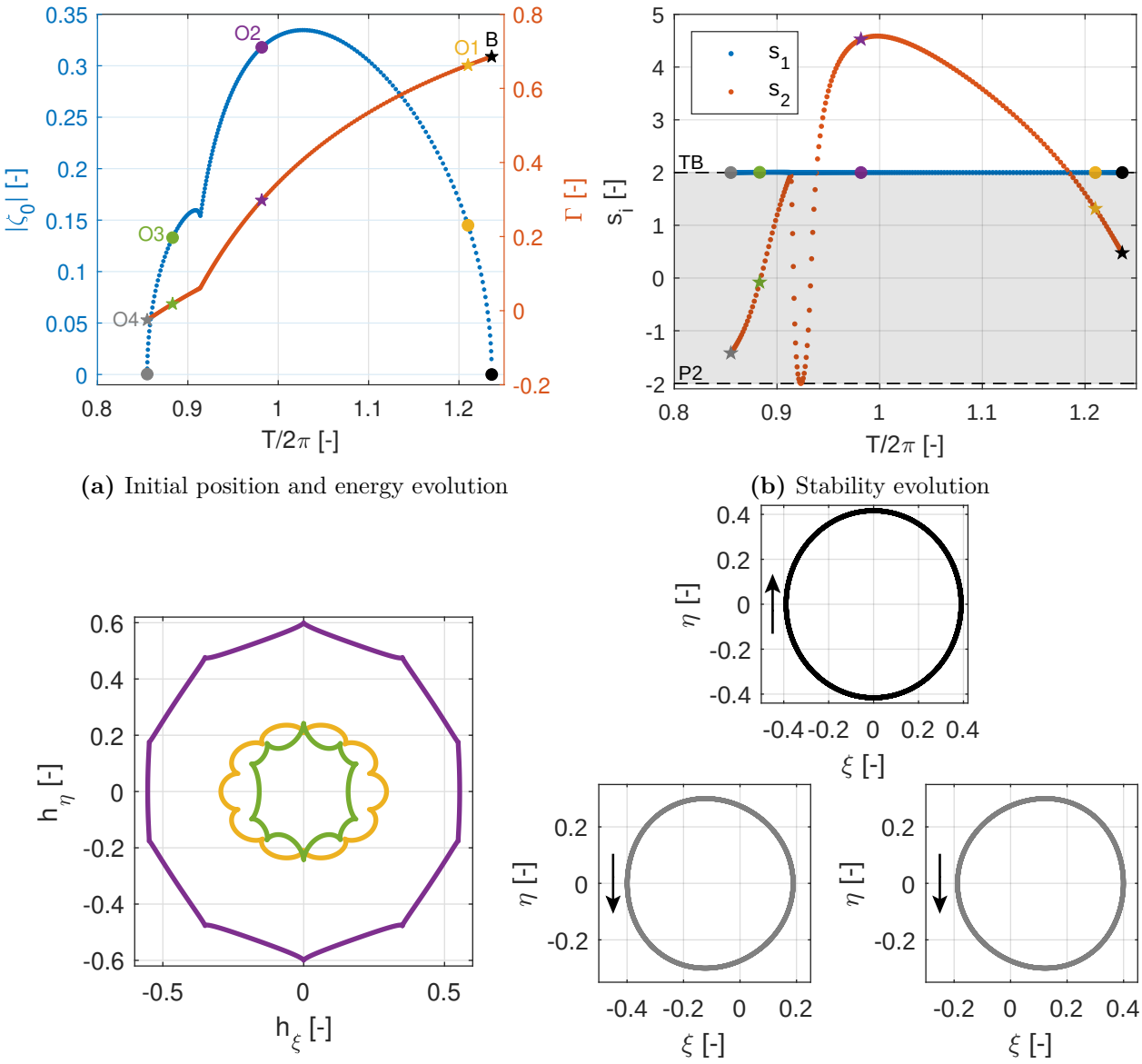

(a) Initial position and energy evolution

(b) Stability evolution

(c) Marked QSOs' rotating angular momentum

(d) Planar marked orbits.

Figure 5.35: High-energy 3D-P6QSO$_2$ family in the H3BP

'O3' orbit, before coming back to the plane with 'O4'. As for the planar projection of the rotating angular momentum, for the 'O1' orbit it is similar to what has been seen before. However, for the other two orbits, the shape changes with the arcs first being inverted for 'O2', and then becoming almost linear trajectories in 'O3'.

The last 3D family studied is the 3D-P7QSO$_2$ family depicted in Figures 5.37 and 5.38. Following the expected trend, this family is composed by two branches, one of northern branches and the other of southern ones, both composed by DS QSOs. This family has a very similar behavior to the previous family, including the fact that it starts from a steady QSO and ends in a planar prograde orbit. However, this time, the prograde orbit belongs to the distant prograde orbit (DPO) family that corresponds to the g family of Hénon [25].

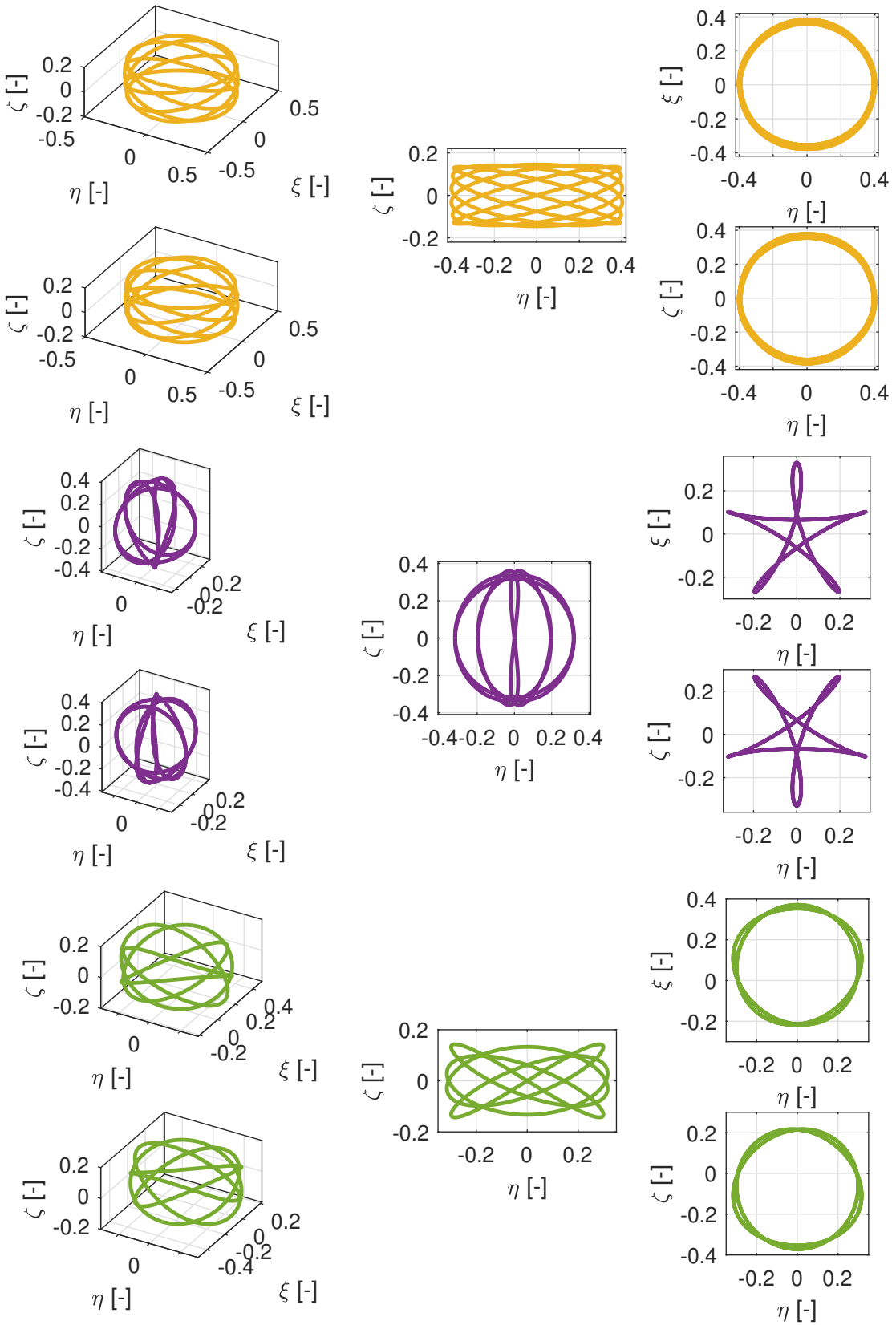

Figure 5.36: Marked 3D orbits of the high-energy 3D-P6QSO$_2$ family in the H3BP

In addition, this time the connection between this family and the DPO family is achieved through a period-sixtupling bifurcation. This follows the trend observed for the two previous families where in the transition from retrograde to prograde motion, two of the loops disappear. Apart from this, the rest of the characteristics of this family follow the same evolution as the previous family, represented by the three marked orbits shown in Figure 5.38 (both the southern and northern version of each orbit).

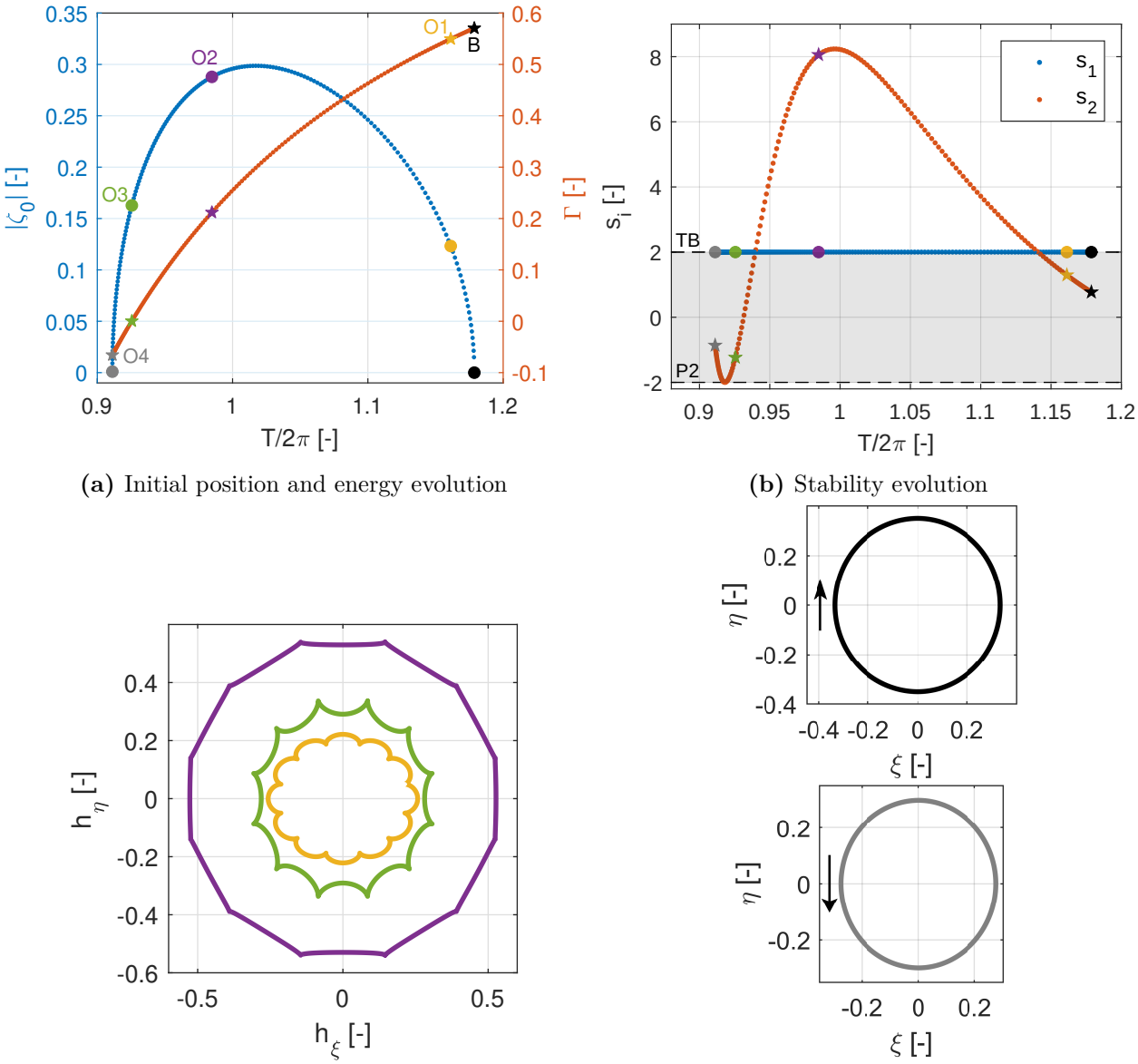

(a) Initial position and energy evolution

(b) Stability evolution

(c) Marked QSOs' rotating angular momentum

(d) Planar marked orbits

Figure 5.37: High-energy 3D-P7QSO$_2$ family in the H3BP

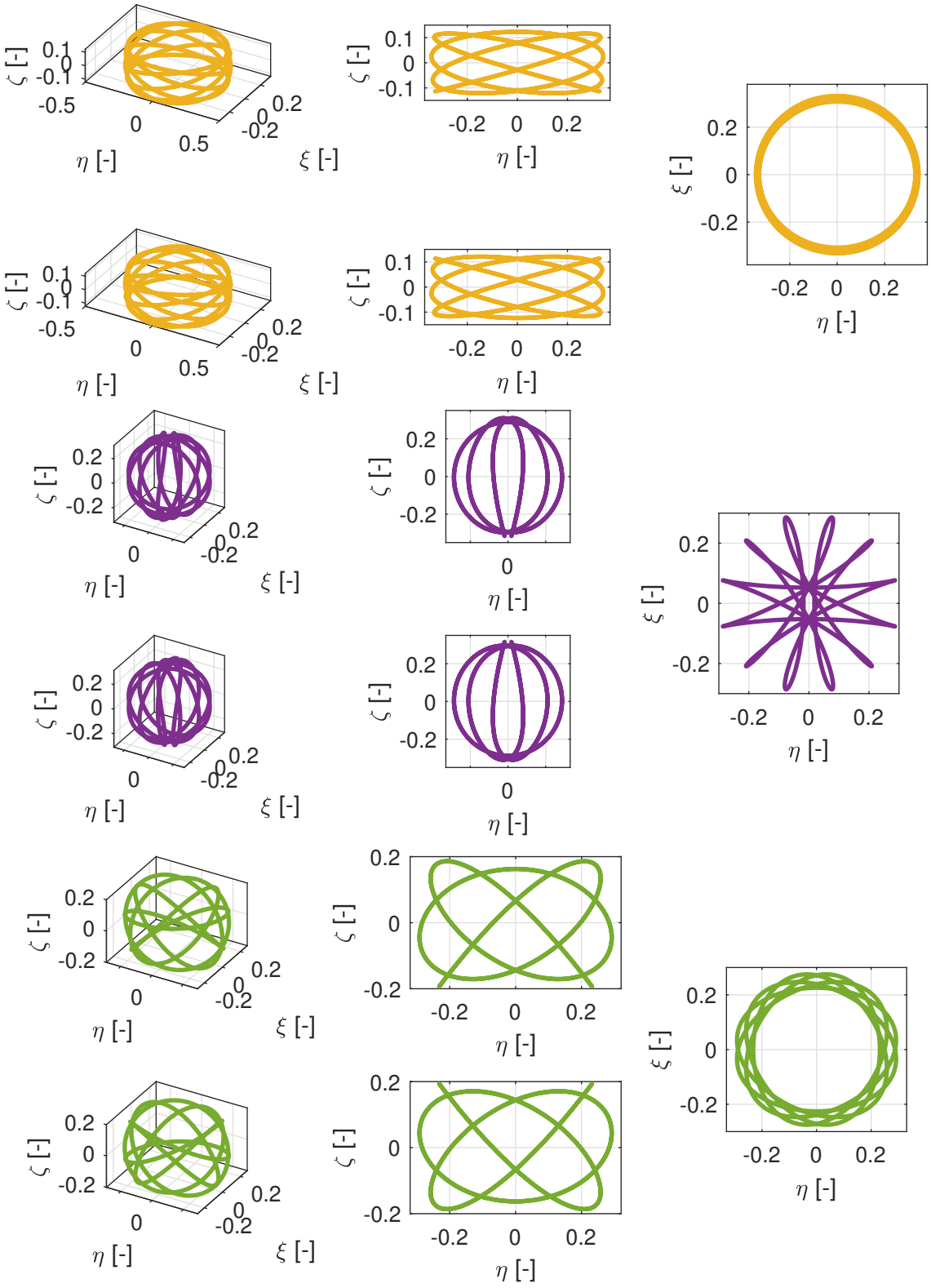

Figure 5.38: Marked 3D orbits of the high-energy 3D-P7QSO$_2$ family in the H3BP

Chapter 6

Planar Quasi-Satellite Orbits in the Circular Restricted Three-Body Problem

Following the study made on the previous chapter of QSOs in the H3BP, in this chapter these orbits are studied but in the most complex CR3BP. However, in this case, only planar orbits are studied. Due to the circular nature of this model, like it happened in the H3BP, in the CR3BP periodic orbits organized in families of orbits. Unlike the H3BP that was a generic model, the CR3BP is a μ-dependent model. Therefore, in the CR3BP different results are obtained depending on the system studied, and the orbits for each of them must be computed separately. In this work, four different systems are studied: Mars–Phobos, Sun–Mars, Jupiter–Europa and Saturn–Titan. In this chapter, the goal is to study the evolution of the families of all of these systems. Nevertheless, as all of them have a small mass ratio, the characteristics of the QSOs are similar in all of them, as can be observed below. Therefore, instead of studying in depth all of the families in all of the systems, only the relevant cases will be studied. In addition, thanks to the small mass ratio of the systems, the H3BP is a sufficiently accurate approximation, which means that the general evolution is the same one as that of the CR3BP. In this sense, this chapter focuses on the differences that exist in the results between the two models.

6.1 Family of Steady QSOs for Different Systems

As mentioned, in this work four different systems are studied: Mars–Phobos, Sun–Mars, Jupiter–Europa and Saturn–Titan. The main characteristics of these systems are shown in Table 6.1. For the CR3BP, the mass ratio μ, the semi-major axis a, and the period, T are required. In addition, the eccentricity e is also included in the table for two reasons. First, it is useful to know how far each system deviates from the circular assumption, and second, it will be needed in the following chapter when using the ER3BP model. Moreover, the mean radius of the second primary is also shown, as it will be necessary later to determine the distance between the orbits and the surface of this body. The four systems studied here

System	$\mu\,[-]$	$e\,[-]$	$a\,[km]$	$T\,[days]$	$\bar{R}_S\,[km]$
Mars–Phobos	$1.661026 \cdot 10^{-8}$	0.0151	$9.3772 \cdot 10^{3}$	0.319087740	11.3
Sun–Mars	$3.227155 \cdot 10^{-7}$	0.0934	$2.279392 \cdot 10^{8}$	686.9715763	3389.5
Jupiter–Europa	$2.528582 \cdot 10^{-5}$	0.009	$6.709 \cdot 10^{5}$	3.550439314	1560.8
Saturn–Titan	$2.366992 \cdot 10^{-4}$	0.0288	$1.221865 \cdot 10^{6}$	15.94622055	2574.7
Earth–Moon	0.0121505	0.0549	$3.84403 \cdot 10^{5}$	27.28485503	1737.4

Table 6.1: Mass ratio μ, eccentricity e, semi-major axis a, orbit period T and secondary mean radius $\bar{R}_S$ of various planetary systems.

have a small μ value. Because of this, the Hill approximation used in the previous chapter provides a good starting point for all of them. However, among the four systems the μ value vary considerably, so it is important to study how this affects the evolution of the families and whether the H3BP model is actual applicable in all the cases. For that reason, in this section the family of steady QSOs is analyzed for all four systems and compared with its H3BP counterpart.

Figure 6.1 illustrates the QSO family for the four mentioned systems: Mars–Phobos (MP), Sun–Mars (SM), Jupiter–Europa (JE) and Saturn–Titan (ST). Both for the energy, (a), and the stability, (b), the four systems have almost the same values. In addition, for these two characteristics are similar to those of the H3BP QSO family. In the case of the stability indices, this similarity between the models is very important as it implies that the bifurcating points take place at the same orbits, which is necessary to have similar swing families as the ones already studied. If these figures were studied zooming the energy and the stability indices, some differences could be observed. These differences to the H3BP references are higher, the higher the value of μ of the system. However, these divergences are small enough to be negligible. Regarding the initial position, which is related with the size of the orbits, it varies depending on the system. In this way, the orbits (in non-dimensional units) increase in size with μ.

Finally, Figure 6.1c shows some of the orbits of the family for each system in the LVLH rotating frame, colored by their Γ value. For this purpose, the orbits are transformed from curvilinear coordinates to Cartesian coordinates in the $\mathcal{L}$ frame, as detailed in Appendix A. This transformation is also applied to all subsequent trajectory figures in the work for both the CR3BP and the ER3BP. A the comparison of the four sets in the figure reveals that, for the Saturn–Titan and even the Jupiter–Europa systems, the curvature of the orbits is very noticeable, especially for the orbits with the highest energy, whereas for Mars–Phobos and Sun–Mars systems, it is almost imperceptible. The difference is mainly due to the varying sizes of the orbits in each system. For example, for $\Gamma \approx 6$, the minimum distance to the primary is about 0.7 for Saturn–Titan but about 1 for Mars–Phobos. As a result, the influence of the primary differs significantly between those two cases. Nonetheless, it is important to note that none of these families is symmetric with respect to the y-axis, even if it looks like it when μ is really small. It is also evident that the size of the orbits increases with the mass ratio μ, as previously noted. Moreover, the secondary body is not included in this figure or in the similar ones that follow in this chapter. Consequently, some of the orbits shown would, in practice, intersect the secondary body and thus be infeasible. The omission is intentional, as

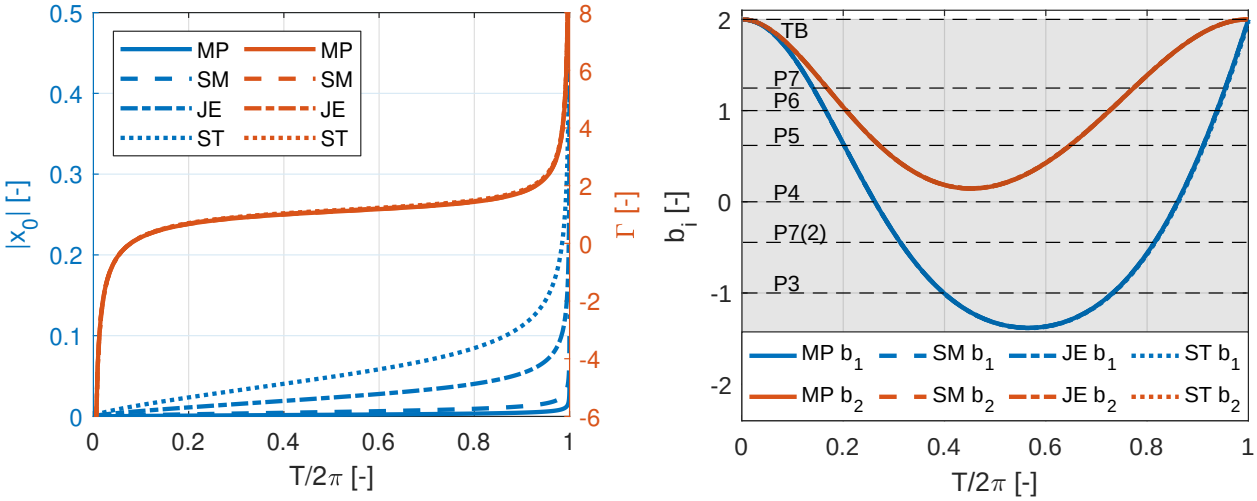

(a) Initial position and energy evolution

(b) Stability evolution with the bifurcation lines

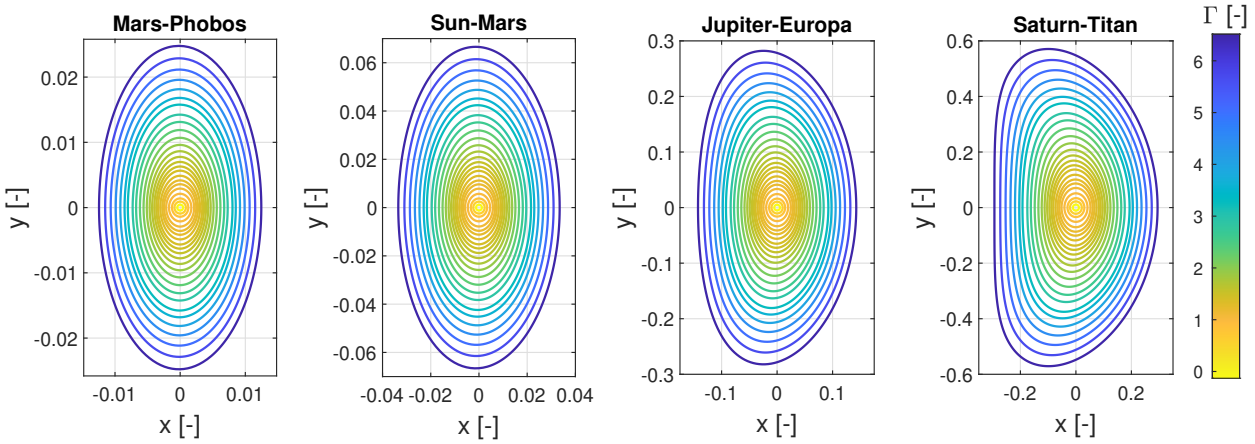

(c) Steady QSO families

Figure 6.1: QSO family in the CR3BP for for various planetary systems

the focus in this chapter is on the evolution of the families and their comparison with the H3BP model. Practical aspects of QSOs, including the relative size of the orbit and the body, will be addressed in the next chapter.

After studying the steady QSO family for the four systems included in this work, one can question how this behavior compares when the μ keeps increasing. For that reason, in Figure 6.2, the family is depicted, but this time for the Earth–Moon system, whose characteristics are also shown in Table 6.1. This system is a very particular planet-moon system, as the mass of the Moon relative to the Earth is big compared with the other natural satellites of the planets of the Solar system. For this reason, the μ value of this system is considerably higher than the other ones studied in here, which made it the perfect example. Starting with Figure 6.2b, where also the QSO family for the Saturn–Titan system is shown for comparison, the first thing that needs to be mentioned is that while for the other 4 systems the period shown was bounded between 0 and 2π, for this system the period reaches values that go a bit beyond 2π. It is important to mention that for the other four systems the period can also be

extended a bit beyond the 1:1 resonance. In fact, the limit asymptotic period is no longer 2π as in the H3BP, but it increases as μ increases. In this sense, for the Mars–Phobos system, this limit is insignificantly higher than 2π, but for the Earth-Moon system the propagation beyond this point plays an important part, as it will be seen next.

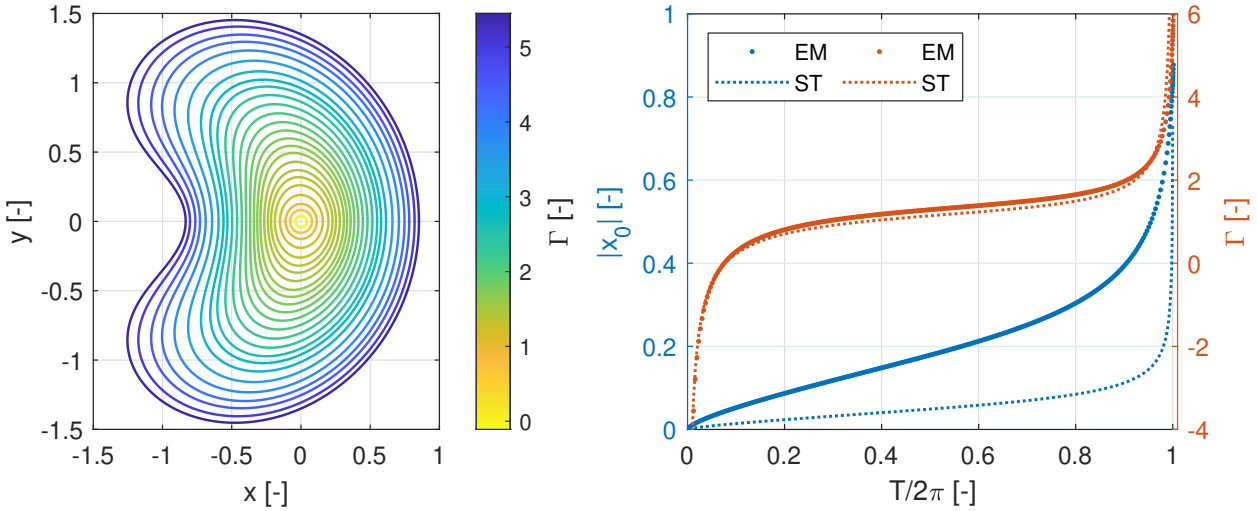

(a) Steady QSO family **(b)** Initial position and energy evolution

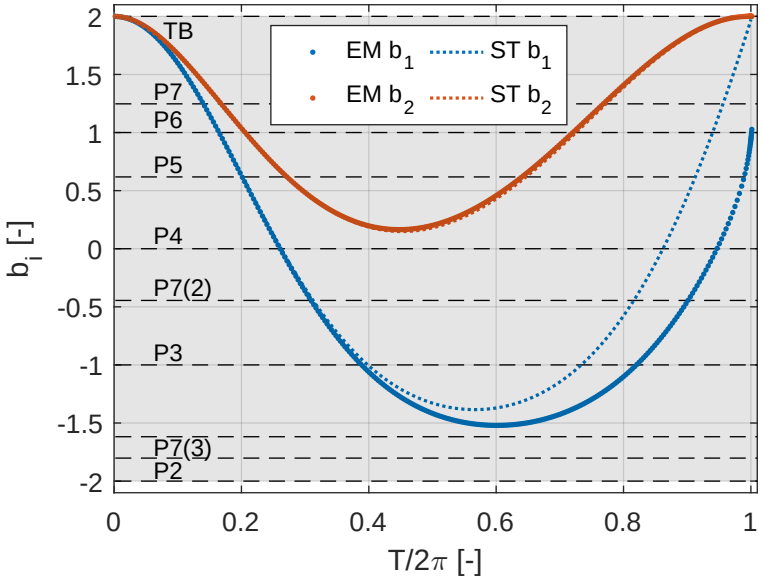

(c) Stability evolution with the bifurcations lines

Figure 6.2: QSO family in the Earth–Moon CR3BP

Keeping the focus still on the same figure, the next thing that is important to notice is that the Γ values are more limited, even if the period is more extended than in the other four systems. Finally, the size of the initial position is bigger, as expected. This translates to a shape of the orbits, specially for high values of energy, much more influenced by the primary and with a high curvature, as illustrated in Figure 6.2a. However, the most relevant change is in the stability indices, more precisely, the in-plane index. Whereas the out-of-plane index has a very similar behavior to those of the other four systems , with a slightly higher value,

the in-plane index diverges a lot from the other 4 cases. For the low-energy low-period part of the family, the Earth–Moon and the Saturn–Titan lines for this quantity are almost the same. Nevertheless, they start diverging right after the first period-tripling bifurcation, and the gap grows as the period increases. The consequence of this difference is that the bifurcations after this take place for a higher period in the Earth-Moon system, as the value of the index remains lower. Not only that, but also, the last period-septupling bifurcation is never reached for this system and the high-energy period-sixtupling bifurcation is reached right at the end of the family. This will have big consequences on the evolution of the high-energy swing families that will be very different from the ones of the four systems included in this study. However, the study of these families is out of the scope of this work.

6.2 Families of Swing QSOs

In general, the swing families within the CR3BP for small values of μ, as the ones of the systems studied in this work, are similar to those of the H3BP. For this reason, instead of restudy all of the families already studied in the previous chapter, only the cases that are different from the H3BP behavior will be studied in this section. In addition, as observed in the previous section with the Steady family, the differences in the family evolution between the 4 different systems included in this work are minimal, so only the families for the for the Jupiter–Europa system will be studied as an example. The reason for choosing the Jupiter–Europa system to showcase the particularities of the swing families in the CR3BP is for its intermediate μ value. A very small μ, such as the one of Mars–Phobos, makes the orbits appear symmetric with respect to the y-axis even though they are not because of the curvature effect. On the other hand, the bigger the μ is, the more relevant the Hill's approximation remains. Therefore, the Jupiter–Europa system is a good compromise.

6.2.1 Symmetric Swing Families: Broken Bifurcations

In general, symmetric families in the CR3BP behave in a similar way as they did in the H3BP. The main difference between the H3BP and the CR3BP is that the first has a doubly symmetry, with respect to the x-axis and the y-axis, while the CR3BP is only symmetric with respect to the x-axis. This brings the first difference that could be noticed between the H3BP steady family and the CR3BP ones, that is the curvature that the latter possesses. Therefore, the doubly-symmetric swing orbits found in the H3BP are no longer doubly-symmetric. However, these orbits, and the families to which they belong, are still classified as doubly-symmetric, as established before. In addition, the shape of the doubly-symmetric orbits still resemblances that of their H3BP equivalent, but with the mentioned added curvature. As for the single-symmetric orbits, they still have a left and a right version, but they are no longer a perfect mirror with respect to the y-axis due to the loss of this symmetry. Another consequence of this is that the families composed by single-symmetric orbits no longer have two completely equal branches, the one of LSS and RSS, as now those two branches have slightly different values of their characteristics, such as energy and stability, although this difference is so small that is usually imperceptible without a big zoom.

As a consequence of this similarity between the H3BP and the CR3BP with small μ values,

except for the special characteristic that some of the symmetric families possesses and that is described next in this section, the distribution of families remains the same, i.e., the families of multiplicity 3, 5 and 7 with order 1 (P3QSO, P5QSO$_1$, P5QSO$_2$, P7QSO$_1$, P7QSO$_2$) are composed of doubly-symmetric orbits, whereas the families of multiplicity 4, 6 and 7 with order 2 (P4QSO$_1$, P4QSO$_2$, P6QSO$_1$, P6QSO$_2$, P7QSO$_3$, P7QSO$_4$) are single-symmetric. Not only the geometrical distribution remains the same, but also, in general, the Γ, period and stability evolution of the families remain pretty much the same as those of the H3BP ones. As for the size of the orbits, which is characterized by the initial distance to the secondary, it varies depending on the μ of the system. However, the evolution is still, in general, the same as that observed in the previous chapter.

These main characteristics mentioned can be observed in Figure 6.3, where the tree of the swing families together with the steady one is illustrated. Like it happened in the previous chapter, to plot all the families of different multiplicity together, the reduced period $T*$ is used. Although in the figure some details cannot be perceived, it can be seen how the general trend is similar to the one observed in the H3BP. The main difference between this figure and the counterpart in the H3BP (Figure 5.3), is that in this one there is no dashed line for the initial position. The reason behind this is just because for the CR3BP, for simplicity, only one of the orthogonal crossings is used, as it will be explained in more detail afterwards.

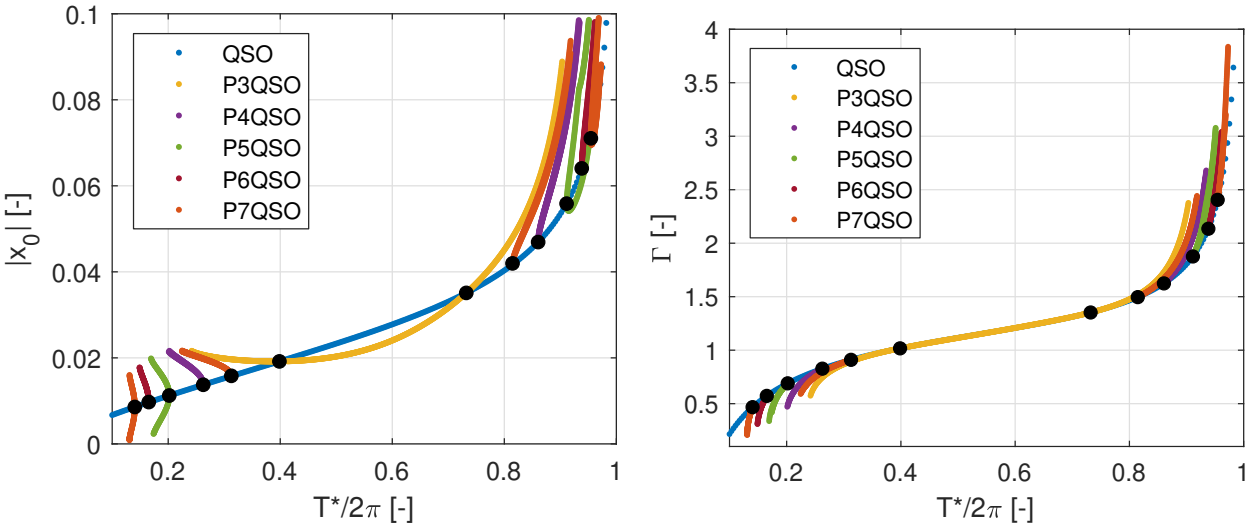

(a) Initial position evolution

(b) Energy evolution

Figure 6.3: Symmetric swing and steady QSO families tree in the Jupiter–Europa CR3BP

In spite of all the similarities between the symmetric swing families in the CR3BP and the H3BP, a phenomenon referred to as "broken bifurcations" in previous works appears for two of the high-energy families, more concretely, for the P5QSO$_1$ and P5QSO$_{1,T}$ and the P7QSO1 and P7QSO$_{1,T}$ families. This phenomenon, where instead of the perfect intersection of normal bifurcations the families are disconnected, has been studied before for different dynamical models, such as the ER3BP [80] and the HR4BP, not only for periodic orbits [81] but also for quasi-periodic orbits [82]. In these studies, the cause behind the destruction of the perfect intersection that leads to broken bifurcation is related to perturbations of the dynamic models

that deform the otherwise pitchfork bifurcation. In the CR3BP, a broken bifurcation has previously been observed in [83] between the families of distant prograde orbits (DPOs) and low prograde orbits (LPOs). In this study, the H3BP is also studied, where there is a perfect intersection between the families that correspond to the g and g' family discovered by Henon [25]. This is exactly the same behavior encountered in this study for the mentioned $P5QSO_1$ and the P7QSO1 cases, and that are studied more in-depth in this section. For further details regarding the origin of broken bifurcations and their characteristics, refer to Seydel [75].

First, let study the family of $P5QSO_1$, depicted in Figure 6.4, and analyze the differences with its H3BP counterpart (Figure 5.7). Similarly to what happened in the H3BP, from the bifurcating orbit 'B' two different branches arise, one with IDS unstable orbits such as the purpled 'O1' and the other with one with EDS stable orbits like the yellow colored 'O2'. At the beginning, the evolution of these two branches is equivalent to that of the H3BP, with similar Γ, period and stability values. Nevertheless, at one point the IDS branch suffers an inflection point, at the grey 'O3', that is reflected, to a greater or leaser extent, in all the characteristics represented in the figure, the initial position, the energy and the stability with respect to the period. In the case of $|x_0|$, the Γ and the out-of-plane stability index, the inflection point does not change the growth direction, but there is just a change in the slope. In the case of the in-plane stability index, there is a local maximum at the 'O3' orbit, after which there is an unstable negative area of the branch. In the unstable area, there is a new minimum at 'O4' and finally, after a brief stable part, the family becomes unstable with an increasing positive index. It is important to remember that in the H3BP this local maximum of the in-plane stability index did not exist, since it kept growing, reaching the positive unstable area directly.

The final and probably the most relevant change that takes place in the inflection 'O3' orbit is a change in the type of orbit. Thus, it can be considered that this inflection point is the start of a third branch. This branch is composed of RSS orbits, like the green 'O4', and, unlike in all the other families that contained single-symmetric orbits, there is no LSS branch. While the first two branches, IDS and EDS, had their counterpart in the H3BP $P5QSO_1$ family, there was no single-symmetric orbit in that family. However, the $P5QSO_{1,T}$ originated through a tangent pitchfork bifurcation from the $P5QSO_1$ was the one composed of single-symmetric orbits and it is where the counterpart of this last branch can be found. Therefore, summing up the relation with the H3BP families: the IDS branch shown in Figure 6.4d corresponds to the IDS branch of the H3BP $P5QSO_1$ family (Figure 5.7e); the EDS branch depicted in Figure 6.4e corresponds to a part of the EDS branch of the $P5QSO_1$ (Figure 5.7d), more concretely, the one located before the tangent bifurcation; and the RSS branch corresponds to the RSS branch of the $P5QSO_{1,T}$ family, which originates from the mentioned tangent bifurcation.

A final consideration that needs to be mentioned again about Figure 6.4 is the position of the initial conditions of each orbit. All the orbits of the family possess two perpendicular crossings to the x-axis, each of them in different sides of the axis. As mentioned with the Steady QSO family, for the continuation, the negative axis perpendicular crossing is used. This is still the case for the swing orbits, in both the single-symmetric and doubly-symmetric orbits. This is another difference with respect to the H3BP, in which both perpendicular crossings

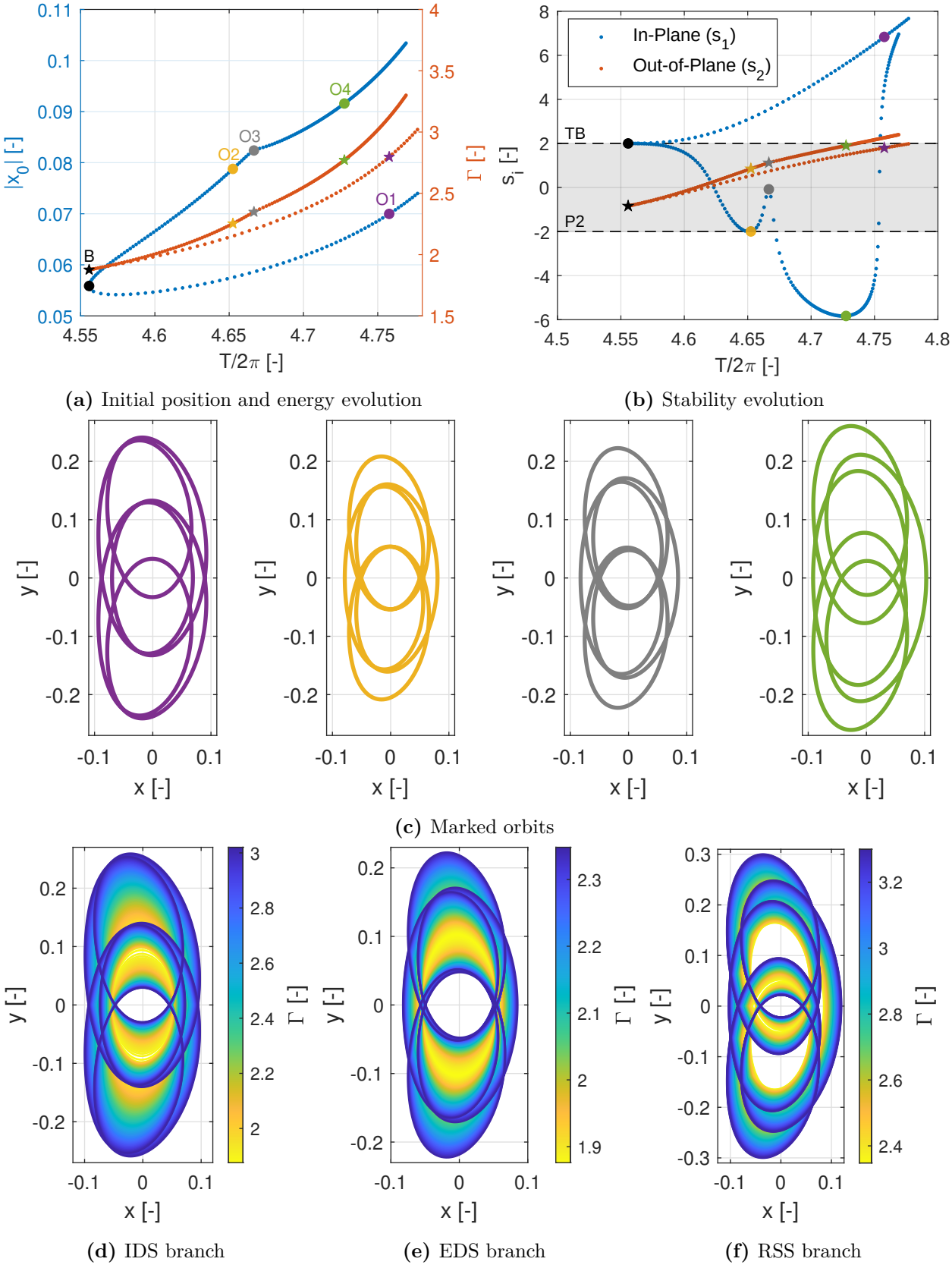

(a) Initial position and energy evolution

(b) Stability evolution

(c) Marked orbits

(d) IDS branch

(e) EDS branch

(f) RSS branch

Figure 6.4: High-energy P5QSO$_1$ family in the Jupiter–Europa CR3BP

were used equally. In the case of the doubly-symmetric orbits, in the H3BP both perpendicular crossings had the same distance to the secondary, due to the y-axis symmetry. However, this is no longer the case in the CR3BP, where depending on which of the perpendicular crossing points is used, the blue dotted line of Figure 6.4a shows slight variations. Therefore, for simplicity, one preferential perpendicular crossing is chosen.

While in the H3BP there was a secondary family originated from a tangent bifurcation, the $P5QSO_{1,T}$, that bifurcation no longer exists in the Jupiter–Europa CR3BP family due to the mentioned critical point. Nevertheless, there still exists a secondary family, which is called $P5QSO_{1,S}$ in this work[1], illustrated in Figure 6.5 and that shares some characteristics with that H3BP family. First, let study Figure 6.5a, where the $P5QSO_1$ family is also included to showcase the concept of broken bifurcation. While in a first look it could seem like there is a normal bifurcation at the grey 'O2' orbit, specially at the energy line, there is actually no bifurcation at all as the two families do not intersect. This figure can be compared to Figure 5.8a, where the actual bifurcation is shown. It can be seen how the different branches of the families are swapped, as the part of the EDS branch of the H3BP $P5QSO_1$ family after the bifurcation is now part of the secondary family. Concretely, the $P5QSO_{1,S}$ family is composed by two branches, separated by the 'O2' orbit. The first is the mentioned EDS branch, exemplified by the yellow 'O1' orbit and illustrated in Figure 6.5d. The second branch, shown in Figure 6.5e and illustrated by the green 'O3', is formed by LSS orbits and has its counterpart within the H3BP in the LSS branch of the $P5QSO_{1,T}$ family (Figure 5.8c). Due to the intrinsic curvature of the CR3BP dynamic model, this last branch is not an exact mirror with respect to the y-axis of the RSS branch of the $P5QSO_1$ family (Figure 6.4f), but it does correspond to the left version of those orbits. This is a very particular situation, as in the single-symmetric primary swing families ($P4QSO_1$, $P4QSO_2$, $P6QSO_1$, $P6QSO_2$, $P7QSO_3$, $P7QSO_4$) the left and right versions of each orbit belong to the same family, as happened in the H3BP.

Now, let study the evolution of the $P5QSO_{1,S}$ family. Starting from the stability evolution (Figure 6.5b), the in-plane pair of eigenvalues of the 'O2' orbit are located at +1, where a change on the stability takes place. This situation corresponds to a tangent bifurcation. However, in this case, no extra family arises from it, as this point corresponds to a fold bifurcation in which there is a minimum in period and energy. As for the two branches, the in-plane stability index for the EDS branch is similar to that of the EDS post-tangent bifurcation of the H3BP $P5QSO_1$ family, i.e. unstable with positive hyperbolic behavior; and the LSS branch has a similar behavior to the RSS branch of the CR3BP $P5QSO_1$ family. Actually, if the stability indices of these two branches RSS and LSS were plotted together, they would be almost superposed except for the area around the grey orbits. The out-of-plane stability index has a similar behavior to the rest of these families for all the orbits of the family, with a slightly higher value of the index for the EDS branch than the LSS one for the same period.

Next, let study the behavior of the energy, period and the initial position 6.5a). As

[1]The change in nomenclature from the H3BP to the CR3BP for this family is made to account for the fact that it no longer come from a tangent bifurcation and to remark the different composition of this family with respect to the $P5QSO_{1,T}$ family.

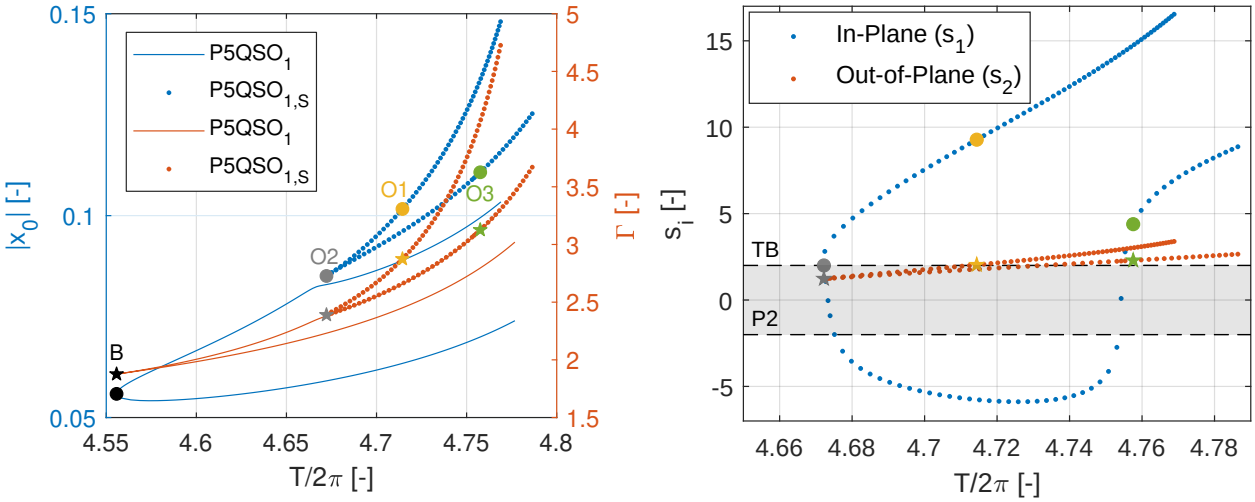

(a) Initial position and energy evolution tree

(b) Stability evolution

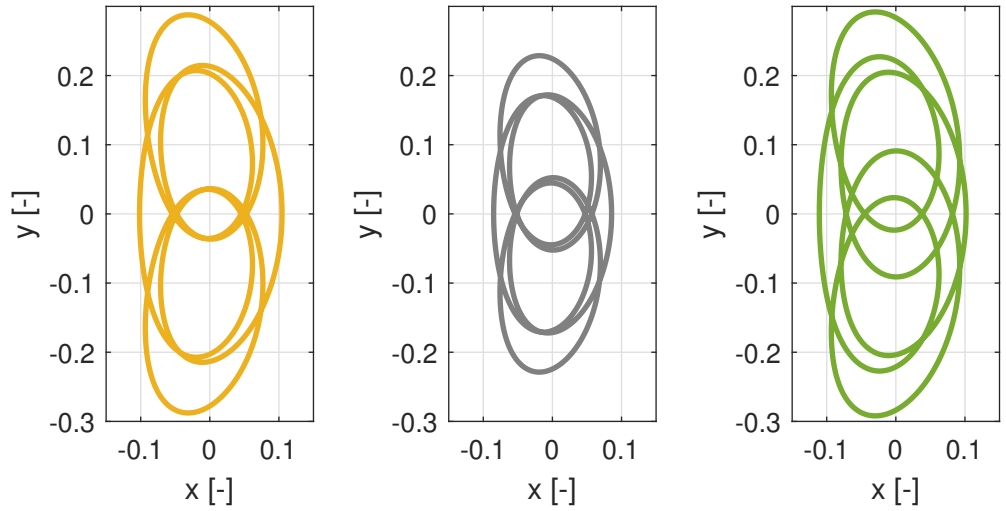

(c) Marked orbits

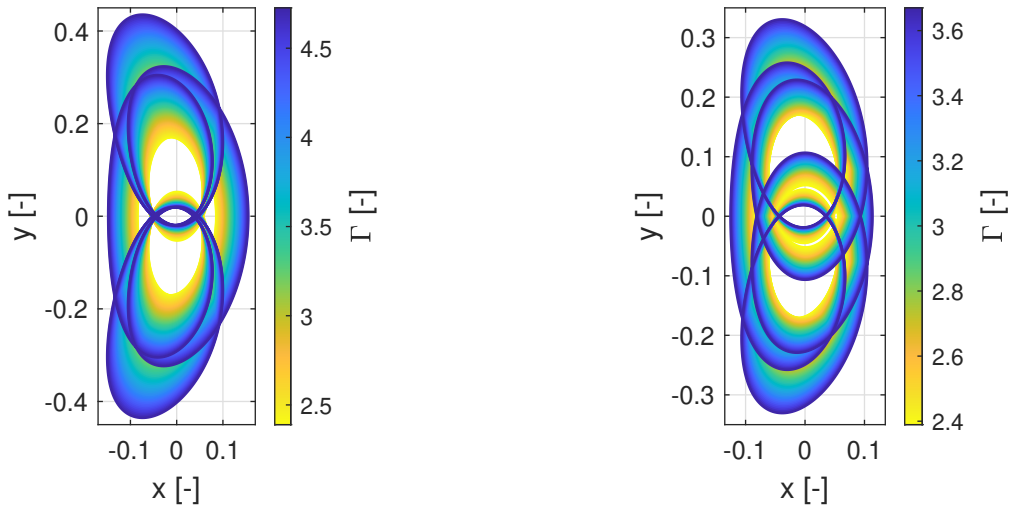

(d) EDS branch

(e) LSS branch

Figure 6.5: High-energy P5QSO$_{1,S}$ family in the Jupiter–Europa CR3BP

mentioned, the 'O2' orbit is a minimum for the period and the energy, and also for the initial distance to the secondary. Comparing both branches, it can be noticed that the EDS branch has a higher energy and a bigger initial distance to the second primary than the LSS branch for the same period. If now the comparison is made between the LSS branch and the RSS branch of the P5QSO$_1$ family, it can be observed that the initial distance is higher for the LSS branch, but the energy of both branches seems to be the same. If the figure were zoomed in for the energy, it would be noticed how the two branches have a tiny gap with the LSS branch, having a bigger energy. Regarding the initial distance, the figure is also misleading, as there seems to be a big gap between the LSS and the RSS branch. Nevertheless, this gap is due to the fact that, as the initial position is placed in the negative x-axis, for the LSS branch this corresponds to the farthest perpendicular crossing, while for the RSS branch it is the closest one. Thus, the big gap observed in the figure is due to this fact and there would be a similar situation to the one of the energy if the same perpendicular crossing was plotted.

As mentioned, the phenomenon of broken bifurcation takes place in both the high-energy $m = 5$ case and the high-energy $m = 7$ cases. For that reason, the next family studied is the P7QSO$_1$ family, represented in Figure 6.6. The comparative behavior of this family with respect to its H3BP counterpart is the same as the P5QSO$_1$ family. The place where in the H3BP family there was a tangent bifurcation, which is the IDS for this family, is now an inflection point at the 'O2' grey colored orbit. This inflection point is a bit more subtle for the initial position than in the $m = 5$ case, but is similar for the energy and the stability indices, where the in-plane one does not reach, again, the value of a tangent bifurcation. Similarly to the $m = 5$ case, the branch after the inflection point is now composed by RSS orbits that in the H3BP were part of the P7QSO$_{1,T}$ family. It is important to remember from the H3BP chapter that, as in this case the single-symmetric orbits derived from an IDS branch, their two perpendicular crossings are placed on the interior part of the orbit. This could complicate the identification of Left and Right orbits visually, as in the CR3BP, due to the curvature, not only the LSS orbits but also the RSS ones usually extend more towards the negative x-axis. For that reason it is needed to compare the orbits with their H3BP counterpart to identify which one is which. Similarly to the Jupiter–Europa P5QSO$_1$ family, the branch in which the inflection point takes place is the one with higher energy and higher out-of-plane stability index.

Finally, the last family studied in this section is the P7QSO$_{1,S}$ family, depicted in Figure 6.7. This family has the same behavior than that of the P5QSO$_{1,S}$, as it is another example of a broken bifurcation. The two branches of this family are the IDS branch, which corresponds to the part of the IDS branch of the H3BP P7QSO$_1$ placed after the tangent bifurcation, and exemplified by the 'O1' orbit, and the LSS branch, whose H3BP counterpart is the LSS branch of the H3BP P7QSO$_{1,T}$ family, is illustrated by the 'O3' orbit. This two branches are divided by the fold-bifurcation located at the grey 'O2' orbit. This turning-point or fold-bifurcation is not actually a bifurcation in the narrow sense of it, as there is no intersection with another family, but it is a point where there is a fold of the family. In this case, the fold bifurcation is a minimum in period, initial position and energy, like it happened with the P5QSO$_{1,S}$. Out of the two branches, the highest-energy one is the IDS branch which is unstable for the in-plane motion. On the other hand, the in-plane stability index of the LSS branch has a more complex behavior that is similar to that of the P5QSO$_{1,S}$ RSS branch. Like in the $m = 5$ case, the

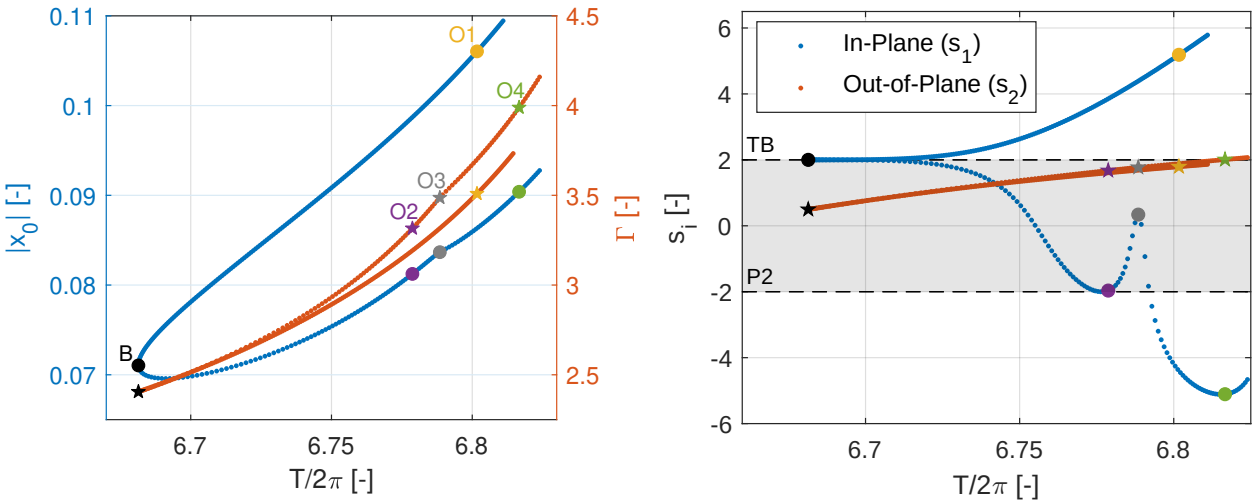

(a) Initial position and energy evolution

(b) Stability evolution

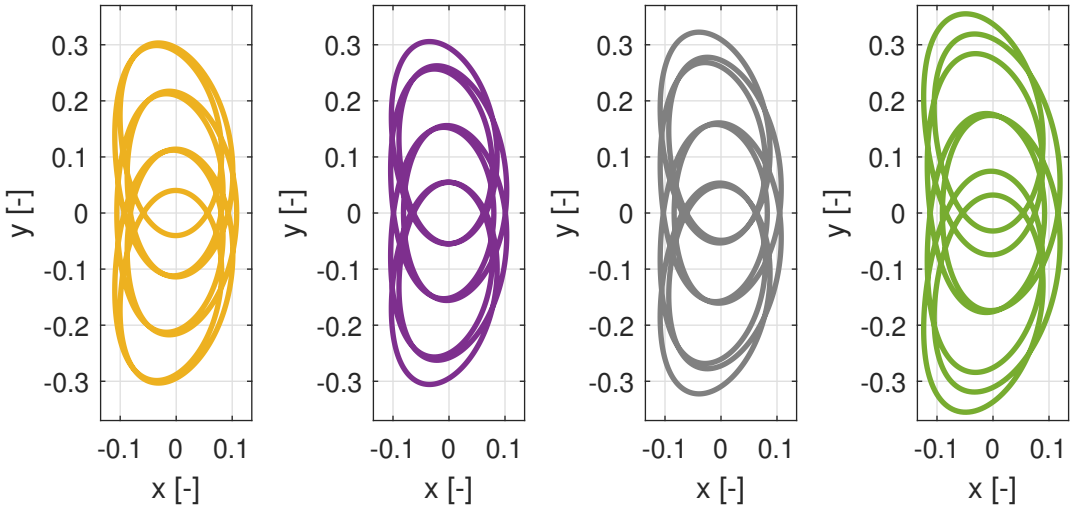

(c) Marked orbits

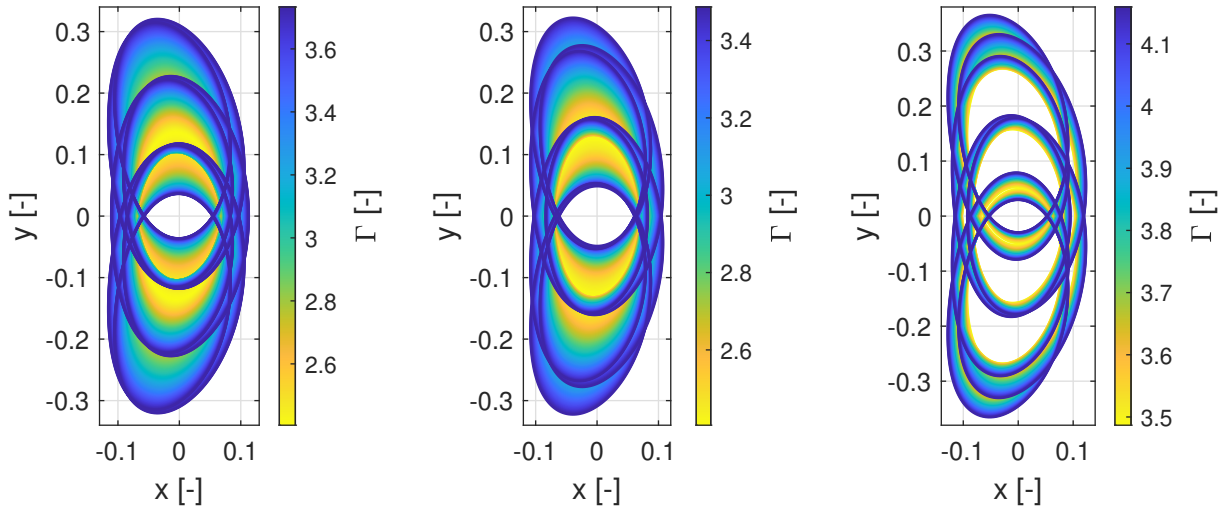

(d) EDS branch **(e)** IDS branch **(f)** RSS branch

Figure 6.6: High-energy P7QSO$_1$ family in the Jupiter–Europa CR3BP

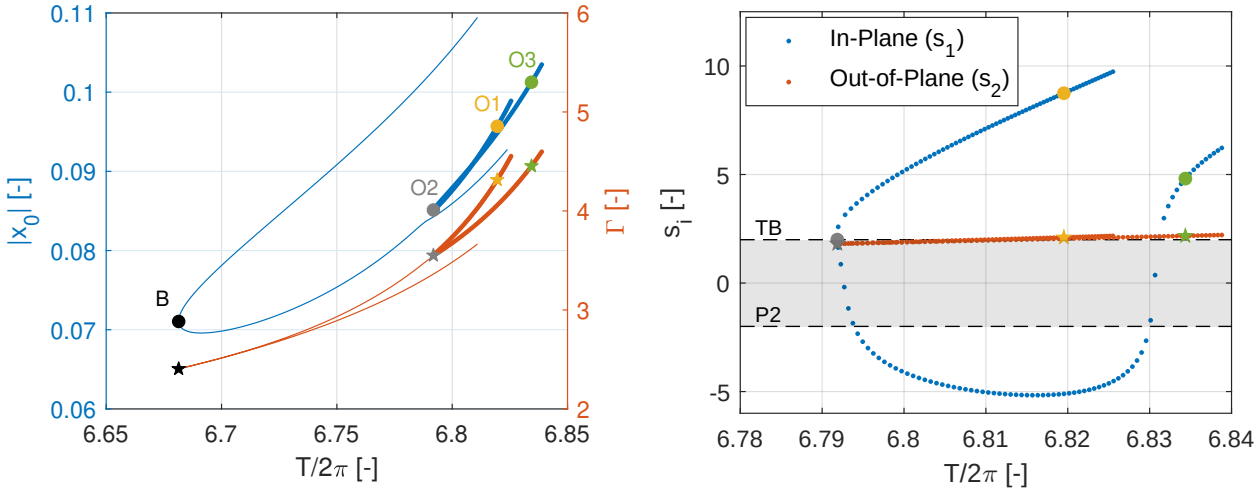

(a) Initial position and energy evolution tree

(b) Stability evolution

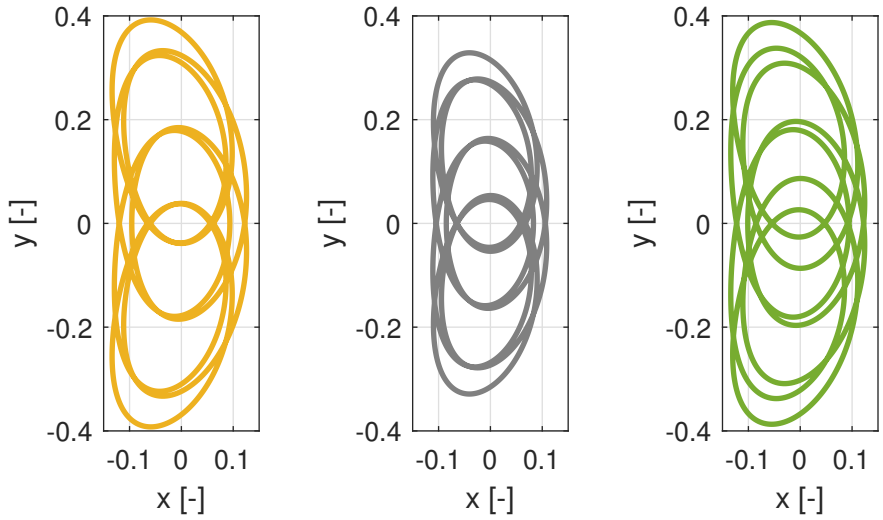

(c) Marked orbits

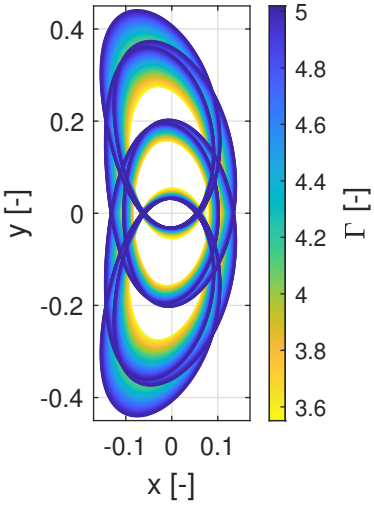

(d) IDS branch

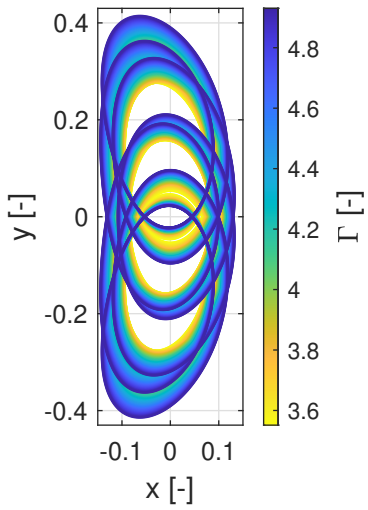

(e) LSS branch

Figure 6.7: High-energy P7QSO$_{1,S}$ family in the Jupiter–Europa CR3BP

energy of the LSS branch of this family is a bit higher than the one of the RSS branch of the $P7QSO_1$ family, even though this difference cannot be appreciated in the figure.

6.2.2 Asymmetric Swing Families

The asymmetric swing families in the CR3BP also share some characteristics with the H3BP ones. However, in this case, the differences are more important than for the symmetric families and, for that reason, all the asymmetric families are studied in this section. Not only that but also the single-symmetric families need to be studied as the main difference of the CR3BP with respect to the H3BP is that the asymmetric families no longer arise from the steady QSO family, but they bifurcate from the symmetric families with which they shared the bifurcating point in the H3BP. This phenomenon can have huge consequences as, even though the trend of the asymmetric families is similar to that of the H3BP families, some of the asymmetric families are now much more limited in period. In fact, there is actually one of the asymmetric families that is no longer found for the Jupiter–Europa CR3BP model.

The second difference that the asymmetric families have with respect to the H3BP does not have major implications for the behavior of the family, but has significant consequences for the continuation process. As explained before, the CR3BP model is not symmetric with respect to the y-axis, unlike the H3BP. For this reason, the asymmetric orbits are no longer symmetric about this axis and are, as their name suggests, genuinely asymmetric. This affects not only the shape of the orbit, but also eliminates the perpendicular crossings that were used for the continuation. As a result, the closure algorithm using the full period of the orbit must be employed. This makes the continuation process more difficult, as the longer propagation time introduces greater numerical error. With this algorithm, a phase constraint must be imposed to fix the location of the initial condition along the orbit. For these orbits, that initial condition is set at a point with $\theta' = 0$. Specifically, this point would correspond to one of the perpendicular crossings used in the H3BP, even though it is no longer a perpendicular crossing. Furthermore, the loss of perpendicular crossings has another drawback: there is no longer a way to enforce asymmetry in an orbit. In the H3BP, since both an asymmetric and a single-symmetric family emerged from the same bifurcating point, an x-axis perpendicular crossing could only be used for the single-symmetric family, and a y-axis one only worked for the asymmetric family. Thus, once the appropriate method was chosen, the desired family could be obtained without difficulty.[2] In contrast, this is no longer the case, and stepping into the new asymmetric family from the single-symmetric one can be tricky. This is especially problematic since the characteristics of the asymmetric and symmetric orbits are very similar. Consequently, although the pseudo-arclength continuation method helps in this process, even with it the continuation may be difficult, and sometimes adjusting the step size is necessary to locate the new family.

Therefore, in the following, all the families, both symmetric and asymmetric, for the multiplicity 4, 6 and 7 with order 2 will be studied, paying special attention to the tangent

[2]In fact, the biggest challenge in the H3BP the steady QSO family. As this family is doubly-symmetric, both continuation algorithms could remain in the steady family when attempting to step into the swing ones. However, this was not a major issue, as the steady and swing families had different enough characteristics that a good initial guess on the direction of the new family ensured successful continuation to the swing families.

bifurcation between symmetric and asymmetric families and to all the other differences that these families have with respect to their H3BP counterparts. Like it was done in the previous chapter, first the high-energy families are studied and then the low-energy ones.

High-energy Families

First, let study the high-energy case of multiplicity 4. For this, the symmetric family that arises from the steady QSO through the high-energy period-quadrupling bifurcation is first analyzed. This is the $P4QSO_1$ family of the Jupiter–Europa CR3BP that is illustrated in Figure 6.8. This family is composed by single-symmetric orbits with both perpendicular crossings in the same size of the x-axis. It has two branches, one formed by LSS orbits (Figure 6.8d), like the 'O1' and the 'O2' orbits, that have the perpendicular crossings located on the negative x-axis, and the second one composed by RSS orbits (Figure 6.8e), such as the 'O3' orbit, and with the perpendicular crossings on the positive side of the x-axis. Previously, it was established that the initial condition would be preferentially located on the perpendicular crossing placed on the negative side of the x-axis. However, this cannot be the discriminatory factor for this family (or for most of the single-symmetric families derived directly from the steady QSO family), as they generally have both perpendicular crossings on the same side. Therefore, the discriminatory factor will be the selection of the exterior perpendicular crossings out of both. As a result, for the RSS, the initial condition lies on the positive x-axis, whereas for the LSS, it is in the negative one.

Taking this into account, first, let analyze Figure 6.8a. At first glance, it appears that there are were two lines emanating from 'B', the bifurcating orbit from which this family arose, for the initial position and only one line for the energy. This recalls the situation of its counterpart in the H3BP, but there are some differences. First of all, in the H3BP the two lines on the initial position corresponded to each one of the perpendicular crossings and both lines corresponded to either branches. However, in this figure only the exterior crossing is considered and each line corresponds to a different branch. Second, in this figure there is actually two different lines for the energy. Nevertheless, they are similar enough to look like superposed. All these differences come from the fact that the LSS branch and the RSS branch are no longer perfectly mirrored, meaning they no longer have exactly the same characteristics. This is a consequence of the asymmetry of the CR3BP model, which gives the orbits a characteristic curvature. Nevertheless, since the μ value for this system is small enough, this effect is limited, hence, both branches are very similar. Another important aspect to highlight in this figure is the fact that both branches arise from the same orbit, the black 'B' orbit. Thus, it is important to not get confused by the fact that there are two black dots, as visible in the zoomed area. Each of these dots corresponds to each of the perpendicular crossings, located at opposite sides of the x-axis. Due to the asymmetry of the y-axis, each of the perpendicular crossings is located at a slightly different distance from the primary. The reason behind showing both perpendicular crossings is that each branch is continued from each of them: the LSS branch from the negative crossing and the RSS from the positive one.

Finally, evaluating the evolution of the initial position and the energy, it can be observed that is similar to that of its H3BP counterpart, excepting the commented difference between branches. Comparing both branches, in the case of the initial position, for the same period,

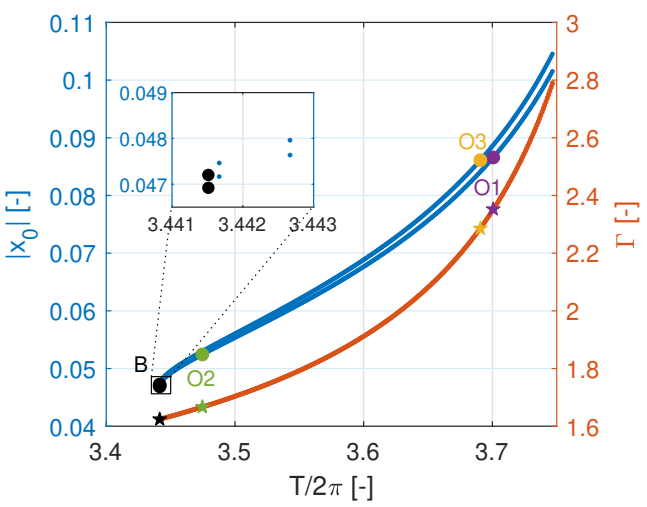

(a) Initial position and energy evolution

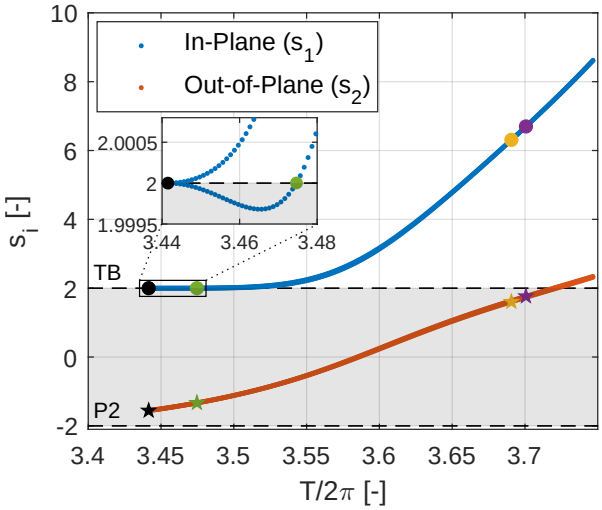

(b) Stability evolution

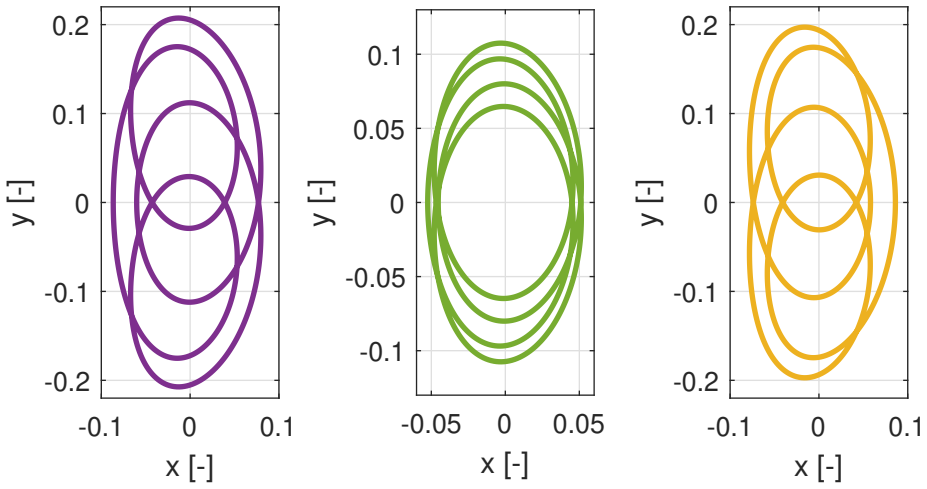

(c) Marked orbits

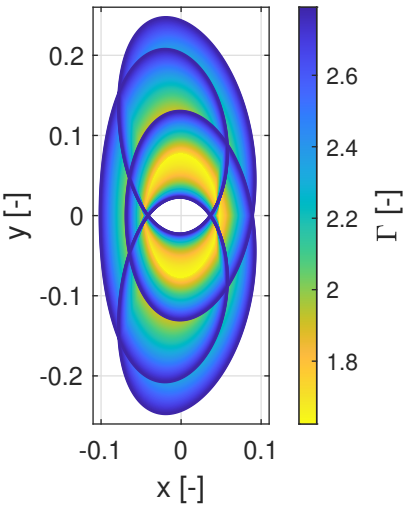

(d) LSS branch

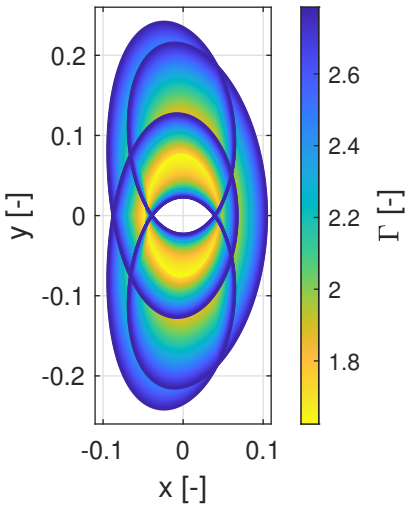

(e) RSS branch

Figure 6.8: High-energy P4QSO$_1$ family in the Jupiter–Europa CR3BP

the RSS branch is a bit farther from the secondary than the LSS branch. In the case of the bifurcating orbit, this implies that its positive perpendicular crossing is at a slightly bigger distance of the primary than the negative one, due to the mentioned asymmetry with respect to the y-axis. As for the energy, the differences are negligible, but the LSS branch has the biggest energy out of the two of them.

The following aspect that needs to be studied from this family is the stability indices shown at Figure 6.8b. First of all, similarly to what happened with the energy evolution with respect to the period, the stability indices of each branch are very similar to the other but with a slight difference. This fact can be observed in the zoomed area, but it is not the reason of this zoom. The zoomed area allows the identification of a tangent bifurcation. This tangent bifurcation will be the origin of the asymmetric $P4QSO_3$ family, as will be seen next. This tangent bifurcation, located at the 'O2' green colored orbit, is located in the branch composed by LSS. This is a very interesting fact, as until now the differences between both branches were insignificant. However, in this case, even though the value of the in-plane stability index at the beginning of both branches has a tiny difference in terms of its value, it has huge consequences in terms of the branches' behavior. While the whole RSS branch is unstable with positive real eigenvalues, the LSS branch is stable at the beginning of the branch for a short interval before becoming unstable like the other branch. Even so, the most important implication is not the fact that some of the orbits of the LSS branch are stable, as the instability of the RSS branch at that stage is negligible. The most important fact, as it was already advanced, is that this change from stable to unstable cause a tangent bifurcation. Out of the formation of the tangent bifurcation, the rest of the evolution of the stability indices of the family is similar to that of its counterpart in the H3BP.

From the tangent bifurcation of the $P4QSO_1$ family, the asymmetric $P4QSO_3$ emerges. This family is reflected in Figure 6.9, which includes 4 subfigures. In Figure 6.9a, both the $P4QSO_3$ and the $P4QSO_1$ families are represented, with the 'B2' orbit connecting them marked in gray. Since the initial conditions for both families are located at a different position along the orbit, they cannot be shown as done previously. For this reason, $|\rho|_{max}$ is used instead of the initial condition for representation. This allows a common plot where the intersection between both families can be observed. In the symmetric family, the maximum absolute value of the ρ coordinate is normally located at the exterior perpendicular crossing, but it can also be located at a different place. However, when it is not located at that perpendicular crossing, the value of this quantity only differs slightly to that of the exterior perpendicular crossing, that is the one used in Figure 6.8a. Hence, the aspect of the plot for this family is the same as the one showed there. As commented before, the asymmetric family bifurcates from the LSS branch of the $P4QSO_1$. This branch was the one with the smallest initial condition. The asymmetric family just after the bifurcation has very similar values of $|\rho|_{max}$ than the LSS branch. Nevertheless, at one point the two of them start deviating, and the asymmetric family starts having bigger values of this quantity than the LSS branch. Not only that, but also it ends having bigger values of $|\rho|_{max}$ than the RSS, when initially it is the other way around. Regarding the energy, the same thing happens. At the beginning of the family, the symmetric and the asymmetric families possess values that are almost identical, but when they evolve, they grow farther from each other, with the asymmetric family having bigger values of energy than the symmetric one.

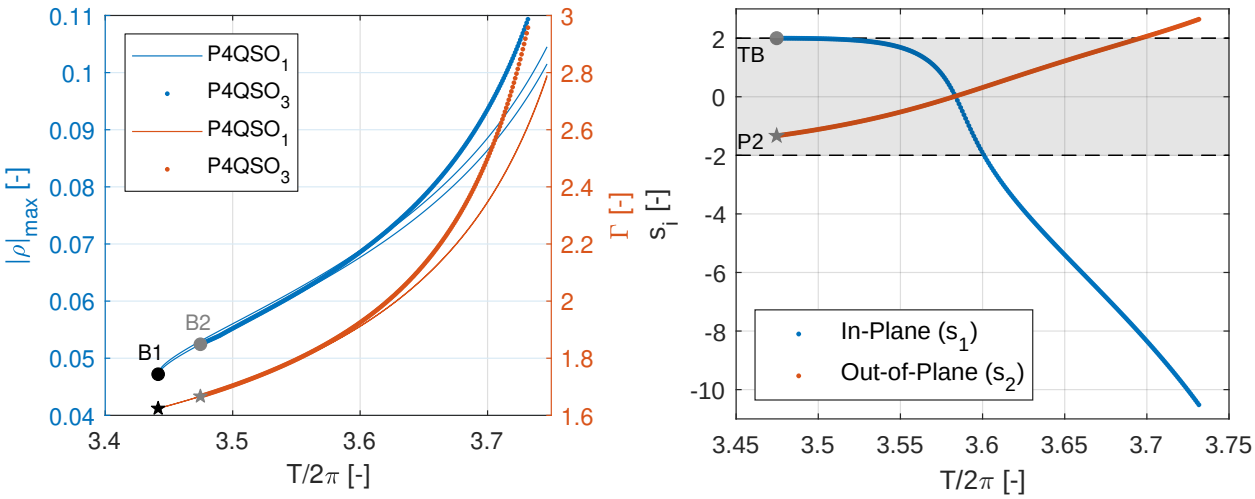

(a) Initial position and energy evolution tree

(b) Stability evolution

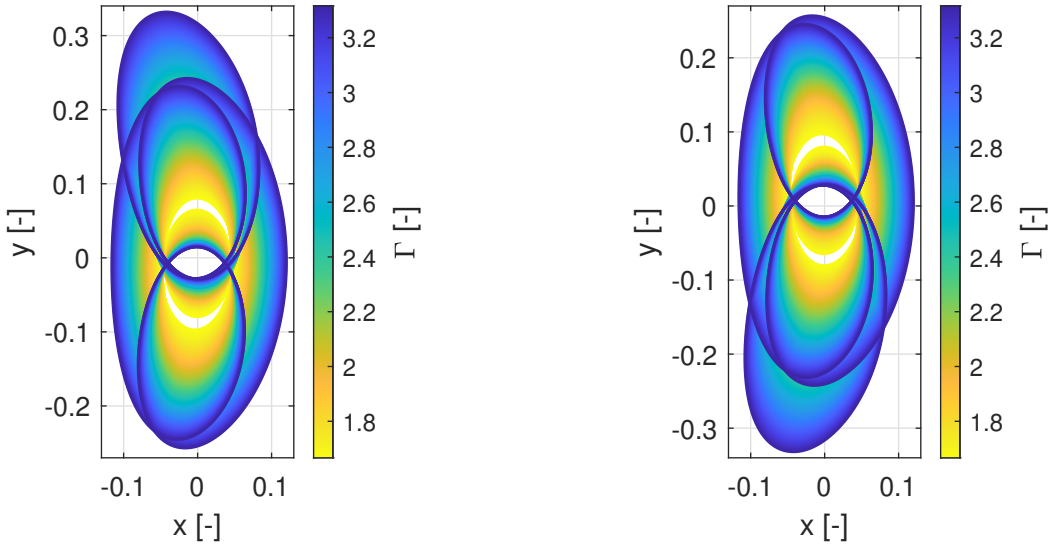

(c) UA branch

(d) DA branch

Figure 6.9: High-energy asymmetric $P4QSO_3$ family in the Jupiter–Europa CR3BP

Once the relation between the symmetric and the asymmetric family is studied, it is important to examine the composition of the asymmetric family by itself. As it happened in the H3BP, the $P4QSO_3$ family is composed of two branches. One of the branches, presented in Figure 6.9c, has UA orbits and the other one, illustrated in Figure 6.9d, is formed by DA QSOs. Contrary to what happened with the single-symmetric families, where in the CR3BP the perfect reflection of their left and right branches was lost, the two branches of the asymmetric families in the CR3BP are still a perfect mirror of each other with respect to the x-axis. The reason behind this is the fact that the CR3BP is still symmetric with respect to the x-axis. As a consequence, the two branches have exactly the same characteristics. Therefore, in Figures 6.9a and 6.9b, both branches of the family are completely superposed and there is a single line for each characteristic. Comparing this family with its H3BP counterpart, it can be observed that all the characteristics of the families are similar, including the stability indices. The

differences are: first, the intrinsic curvature of the CR3BP that all the swing orbits have; and second, the fact that the starting point of the family is different. This last difference has two consequences. The first is that the minimum period of the Jupiter–Europa family is higher than that of the H3BP one. The second is that the starting orbit of the families is different. While in the H3BP this orbit is a steady QSO, in the CR3BP it is a symmetric swing QSO. At the beginning of the CR3BP family, there is a small transition from the shape of the symmetric swing to the common shape of the asymmetric orbits. As a result, the shape of the orbits at the start of the CR3BP asymmetric family is more different than their H3BP counterpart. Finally, as the family is stable right after the bifurcation, for both branches, while the $P4QSO_1$ family was stable before the bifurcation and unstable after it, the tangent bifurcation between them is a supercritical pitchfork.

The next case studied here is the one of the symmetric $P6QSO_1$ family and the asymmetric $P6QSO_3$ one. Figure 6.10 depicts the $P6QSO_1$ family. This family consists again of single-symmetric orbits with both perpendicular crossings at the same side of the orbit. In this sense, the figure has similar characteristics to those of the $P4QSO_1$'s figure. So, the family has two branches, LSS and RSS, that are not a perfect reflection of each other, but have similar characteristics. Like the $P4QSO_1$ family, the RSS branch has a bigger initial distance to the secondary. Nevertheless, this time the branch that has a slightly higher energy is the RSS branch. Another difference that this family has with the one of multiplicity 4 is related to the stability indices. Again, there is one branch that starts being stable and possesses a tangent bifurcation when it becomes unstable. This time, however, that branch is the RSS branch instead of the LSS one. Additionally, this bifurcation happens a bit further from the beginning of the family than in the $m = 4$ case. This has as a consequence that the 'O2' LSS orbit, at which the tangent bifurcation takes place, is more different from the steady orbit, with the symmetric swing motion a little bit more developed than in the previous case.

Figure 6.11 illustrates the $P6QSO_3$ family that bifurcates from the RSS branch of the $P6QSO_1$ family through a supercritical pitchfork bifurcation. Again, the behavior of this family is the same as the one of multiplicity 4. The family consist of two branches that mirror each other: one of UA QSOs (Figure 6.11c) and the other with DA orbits (Figure 6.11d). Figure 6.11a shows how, at the beginning of the family, its evolution closely follows that of the $P6QSO_1$ family, but they later diverge, with the asymmetric family reaching higher energy and a larger maximum ρ distance. In fact, this time the family bifurcates from the branch with the greater $|\rho|_{max}$. Another difference is that, in this case, the evolution of $|\rho|_{max}$ for the symmetric family noticeably differs from that of the exterior perpendicular crossing distance. This is why, in this figure, the two branches of the symmetric family intersect in the blue line, unlike what occurs in Figure 6.10a. As for the stability, Figure 6.11b, it follows the same pattern as that of the $P4QSO_3$ or the H3BP $P6QSO_3$ counterpart.

The last case of the high-energy families is the one of multiplicity 7 and order 2. The symmetric family that bifurcates from the corresponding bifurcating orbit of the steady QSO family is the $P7QSO_3$ one, which is presented in Figure 6.12. This family behaves in the same way as the previous two symmetric families, but it has some differences that will be explained. As in the previous cases, the family is composed of two branches, the LSS branch (Figure 6.12e), represented by the 'O1' purple colored orbit, and the RSS branch (Figure 6.12d),

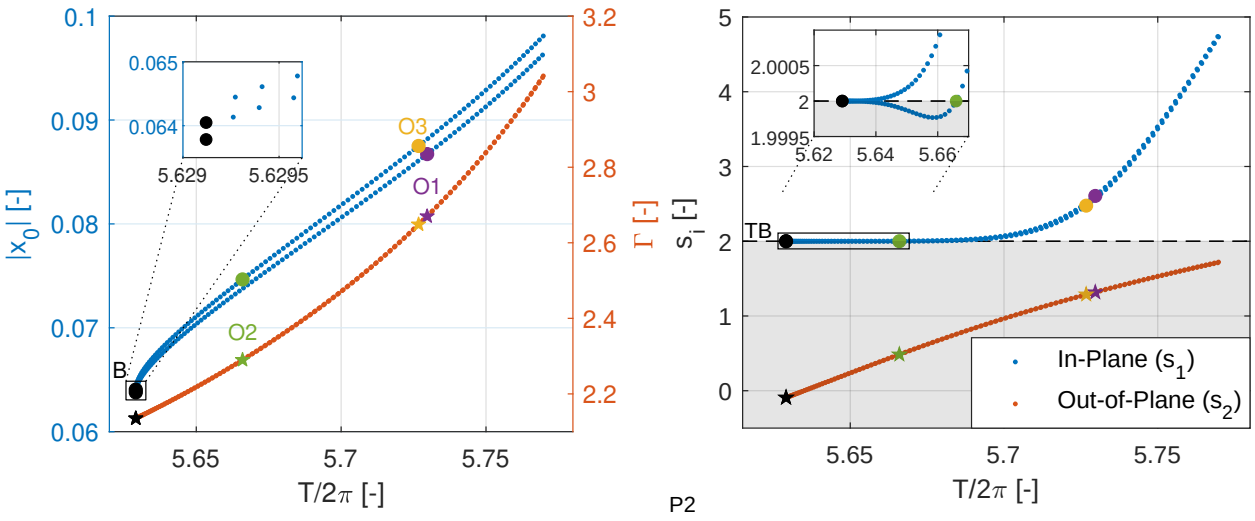

(a) Initial position and energy evolution

(b) Stability evolution

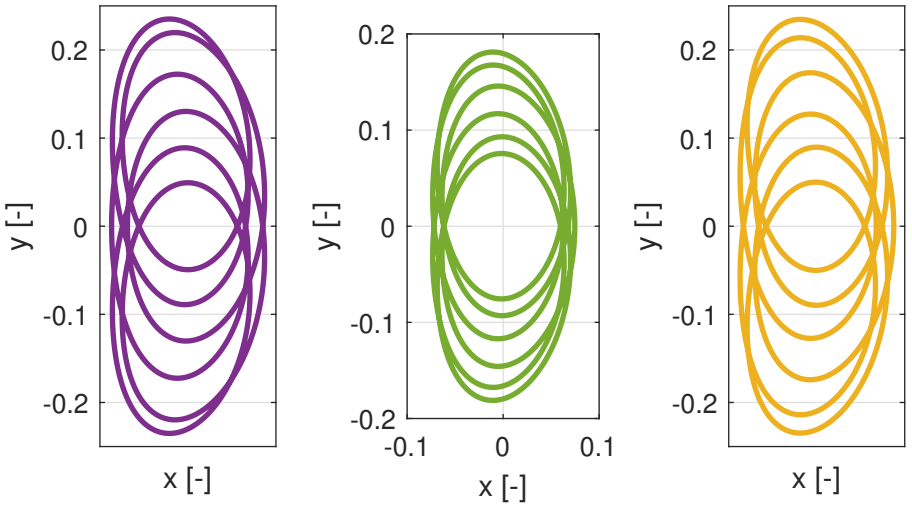

(c) Marked orbits

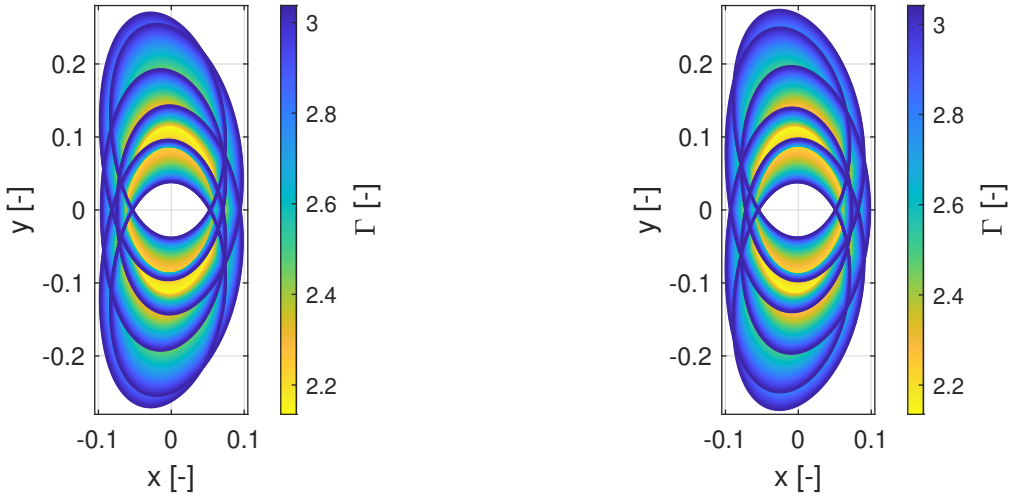

(d) LSS branch

(e) RSS branch

Figure 6.10: High-energy P6QSO$_1$ family in the Jupiter–Europa CR3BP

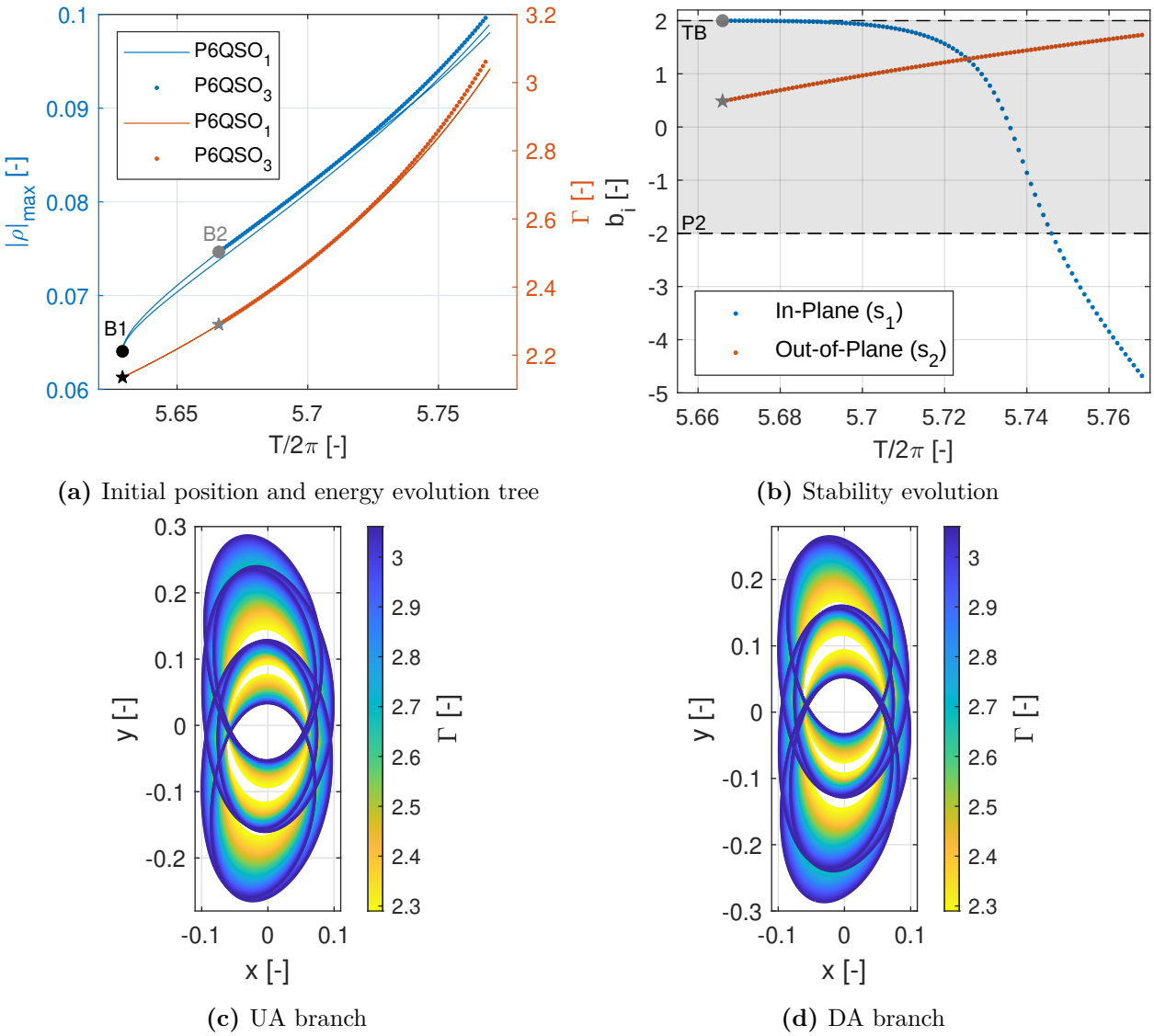

(a) Initial position and energy evolution tree

(b) Stability evolution

(c) UA branch

(d) DA branch

Figure 6.11: High-energy asymmetric P6QSO$_3$ family in the Jupiter–Europa CR3BP

illustrated by the yellowed 'O3' QSO. However, these single-symmetric orbits do not have both perpendicular crossings on the same side of the x-axis, but on opposite sides. The criterion of using the most exterior one of the perpendicular crossings as an initial point within the orbit is nevertheless maintained, to follow the same approach as for the rest of the symmetric families in this section. Among the two branches, the one that has the bigger distance from the initial point of the orbit to the secondary is the LSS branch, which contrasts with the behavior of the two previous families. As for the energy, the branch with the higher energy, even though the difference is almost negligible, is the LSS branch, like in the P4QSO$_1$ family. Moreover, this branch, the LSS, is the one in which the tangent bifurcation is placed following what happened in the $m = 4$ case. Analyzing the behavior of the tangent bifurcation, placed on the 'O2' orbit, some more differences with the previous cases can be seen. First, this time the difference in in-plane stability is a bit more noticeable, as it can be observed in the not-zoomed part of the graphic too. The other difference is that this time the tangent

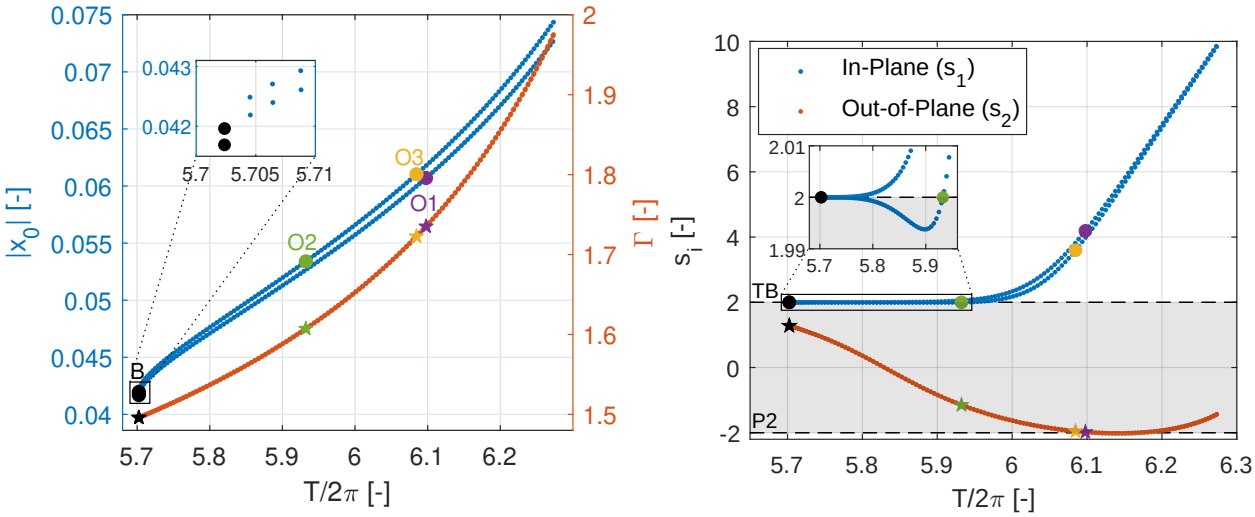

(a) Initial position and energy evolution

(b) Stability evolution

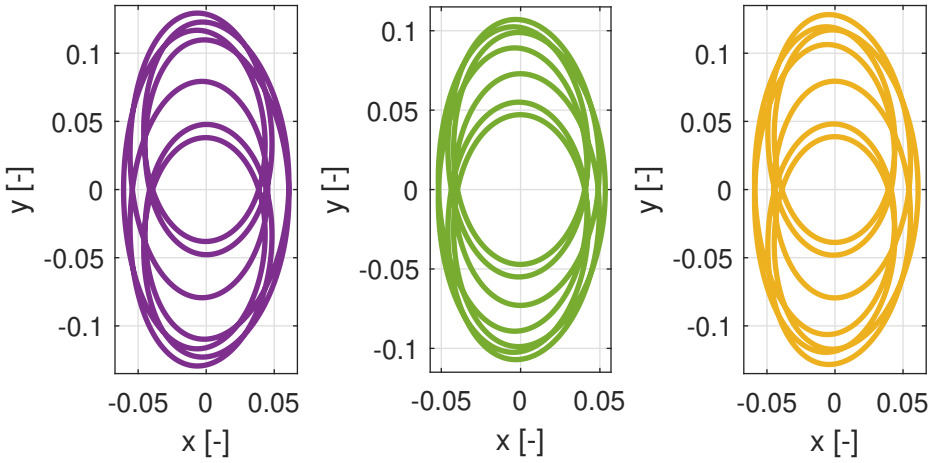

(c) Mixed orbits

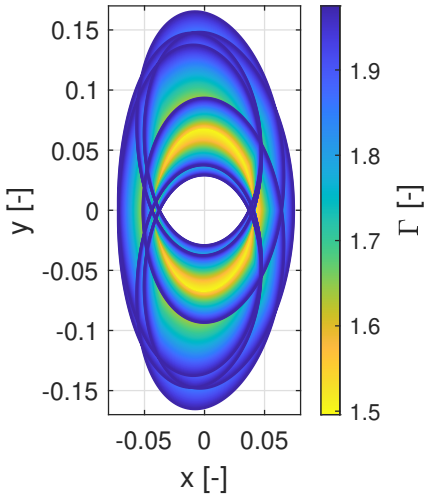

(d) RSS branch

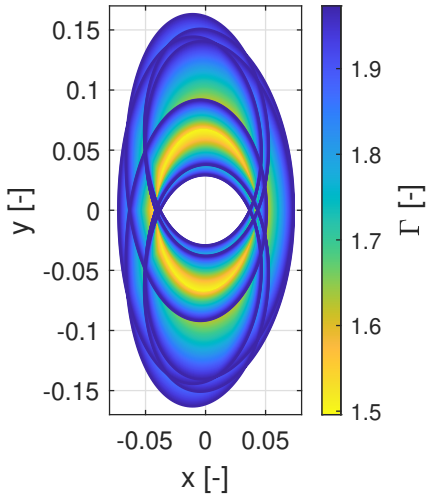

(e) LSS branch

Figure 6.12: High-energy P7QSO$_3$ family in the Jupiter–Europa CR3BP

bifurcation takes place even later in the branch than in the P6QSO$_1$ family. Lastly, it is important to mention that the shape of this family is almost the same as in the H3BP model, as in this family the curvature effect is less noticeable.

Finally, the last family studied in this section is the P7QSO$_5$ family, that is the one bifurcating from the symmetric P7QSO$_3$ family. Like in the two previous cases, this bifurcation is a supercritical pitchfork one, due to the stability behavior of the two families around the bifurcation, and this asymmetric family possesses very similar values on energy and $|\rho|_{max}$ than those of the symmetric family, although they start diverging some as they evolve. Among this divergence, the asymmetric family has the biggest values among both on the two quantities. As for the stability (Figure 6.13b), it is similar to that of its H3BP counterpart family. In addition, the out-of-plane index is like the one of the symmetric P7QSO$_3$ family. Finally, the two branches of the family, the UP and DA branches, are represented in Figures 6.13c and 6.13d, respectively, and are, once again, a mirror of each other.

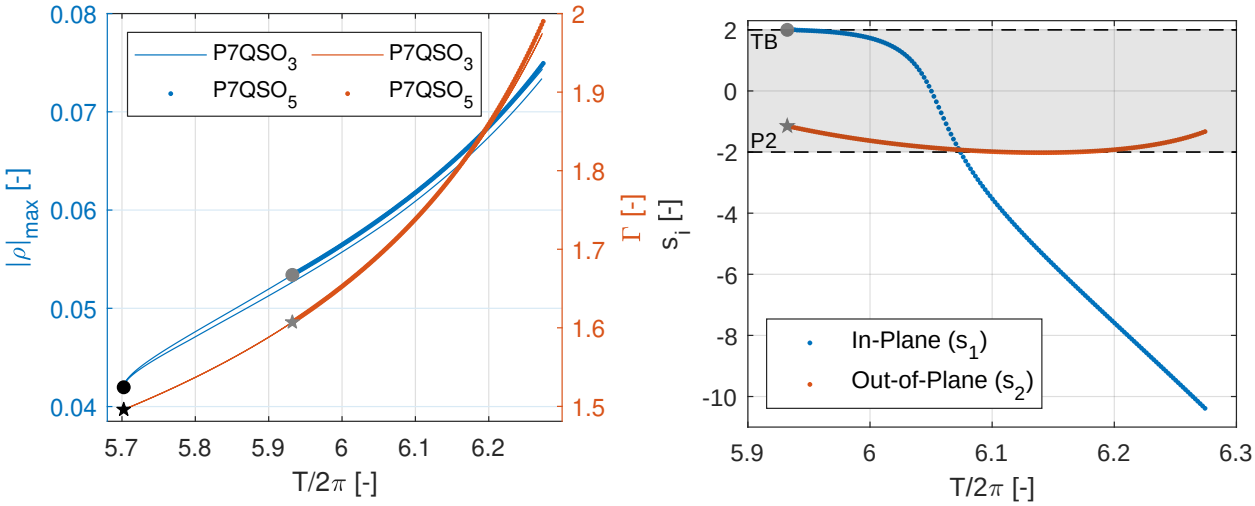

(a) Initial position and energy evolution tree

(b) Stability evolution

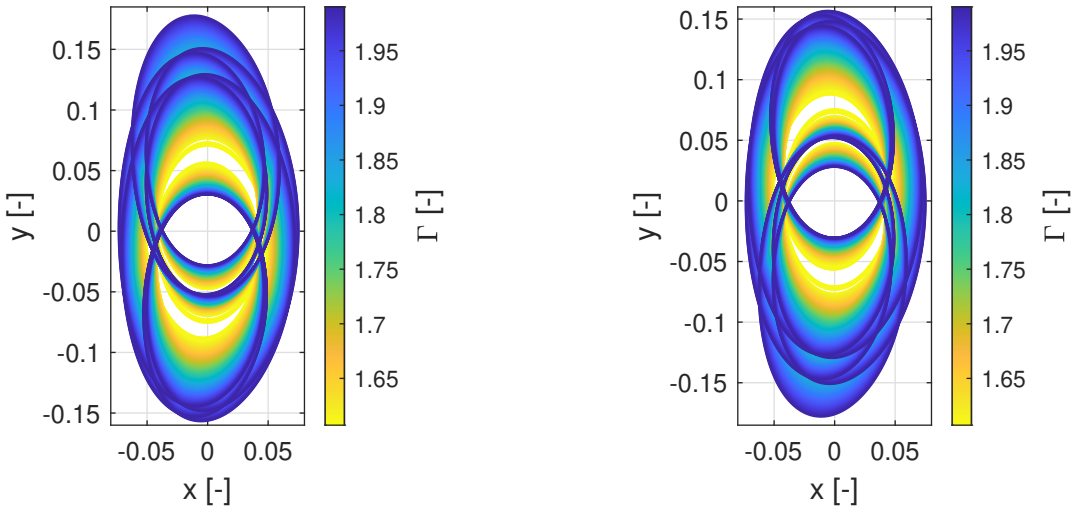

(c) UA branch

(d) DA branch

Figure 6.13: High-energy asymmetric P7QSO$_5$ family in the Jupiter–Europa CR3BP

Low-energy Families

In this section the low-energy single-symmetric and asymmetric families are studied. The first of these cases is the low-energy case of multiplicity 4. Thus, the first family studied in this section is the $P4QSO_2$ family that is presented in Figure.6.14. This family behaves in a similar way to the high-energy symmetric families, but with the typical characteristics of a low-energy family that were studied in the H3BP family and that, in general, are kept in the CR3BP. Accordingly, the family is composed by single-symmetric orbits that possess two perpendicular crossings with respect to the x-axis, each of them located on the same side of the orbit. Again, as the two perpendicular crossings are at the same side of the x-axis, the exterior one is selected to place the initial conditions. The family has two different branches: the LSS branch (Figure 6.14d) and the RSS branch (Figure 6.14e). These two branches are almost a mirror with respect to the y-axis of each other, but with the mentioned effect of the curvature of the CR3BP model. However, due to the smallest size of these orbits, that curvature is smaller and the shape of the orbits is almost the same one observed in the H3BP. This does not mean that the branches are a mirror of each other, as the characteristics of each one are not exactly the same, as it can be observed in Figures 6.14b and 6.14c.

First, on 6.14a, it is observed that out of the two branches the RSS branch is the one with a bigger initial distance to the second primary, as the rest of the single-symmetric families excepting the $P7QSO_3$ one, but the energy is higher for the LSS branch. This last branch is also the one that possesses the tangent bifurcation on the 'O2' green colored orbit, as observed on 6.14b. In this figure, the evolution of the stability indices is illustrated. The out-of-plane index has similar values for both branches as is common in these families. Nevertheless, in this family the in-plane stability index of both branches is for the first time different enough that no zoom is needed to observe the differences. In addition, while for the high-energy families both branches were mainly unstable, with only a small portion of the branch with the bifurcation being stable, that is not the behavior in here. In the H3BP, the low-energy single-symmetric families were stable after the period-multiplying bifurcation from which they emerged. This behavior is more or less kept in here, with the exception of the tangent bifurcation. The RSS branch, where no tangent bifurcation is detected, starts being stable, and after a while it crosses the 'P2' line and becomes unstable with negative hyperbolic behavior. Nevertheless, the LSS branch starts with a small unstable index before reaching the stable area, after which it has the expected trend. This change in stability is what gives rise to the mentioned tangent bifurcation. Another difference with the high-energy orbits is where this bifurcation takes place. Unlike the high-energy symmetric families, the low-energy ones have a limit in a collision. In addition, while in the H3BP the family could be continued past some collisions leading to mixed orbits, in the CR3BP that was not able to achieve, and the continuation was stopped as soon as a collision was closed enough. For that reason, and as in this work the focus is retrograde orbits, this will be considered the limit of the families. Actually, while in the previous section for the high-energy families, only the relevant part of them were shown, in the low-energy ones all the extension of the family is shown. Keeping this in mind, it can be observed how the tangent bifurcation is placed in the second half of the LSS branch. This will have important consequences on the asymmetric family that arises from it.

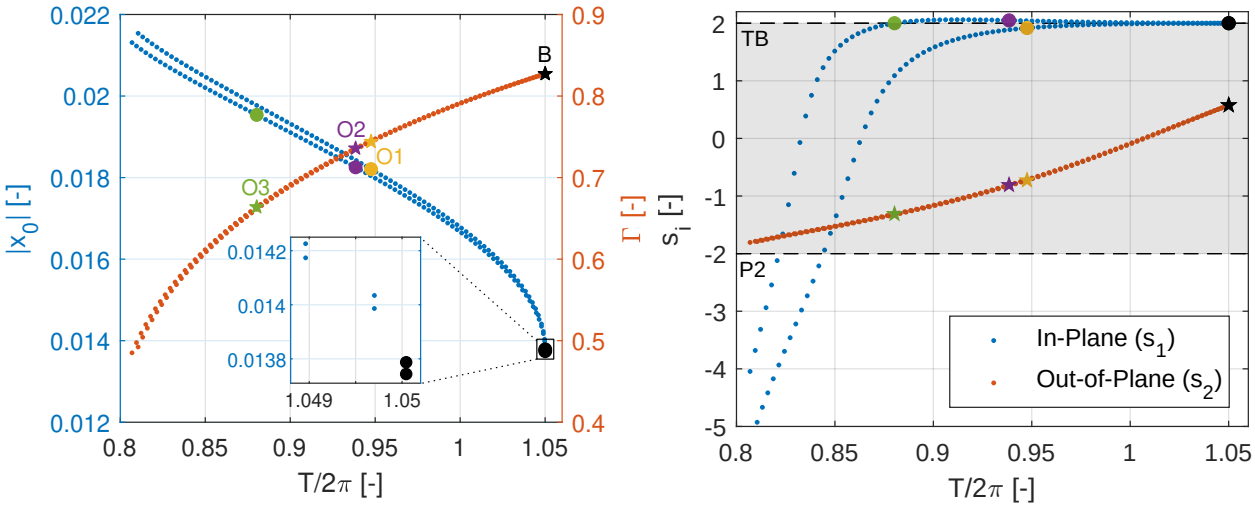

(a) Initial position and energy evolution

(b) Stability evolution

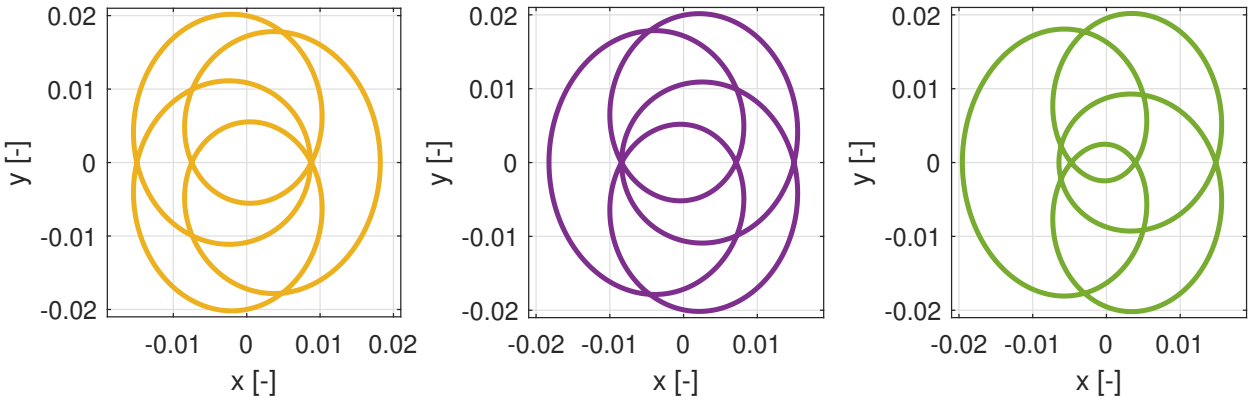

(c) Marked orbits

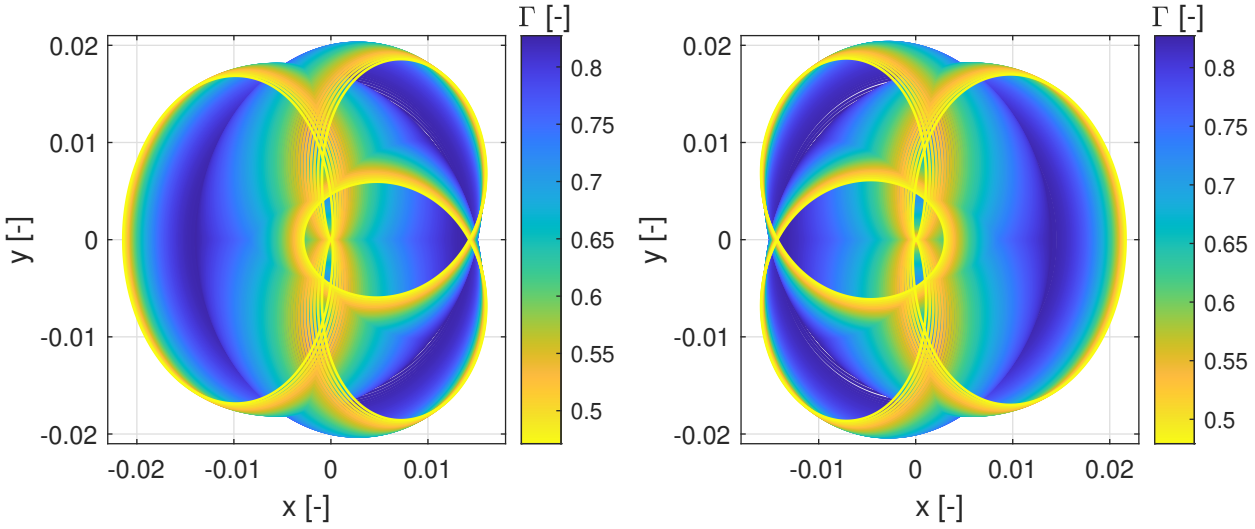

(d) LSS branch

(e) RSS branch

Figure 6.14: Low-energy P4QSO$_2$ family in the Jupiter–Europa CR3BP

From the mentioned tangent bifurcation, the P4QSO$_4$ family is obtained. This family, represented in Figure 6.15 is composed by two branches of asymmetric orbits, as in all the previous cases. However, this time, this family is very different from its H3BP counterpart. The first aspect in which it differs is the extension on the family. As has just been mentioned, the tangent bifurcation from which this family emerges takes place very deep in the symmetric family. For this reason, the origin of the asymmetric family, which indicates the maximum period and energy of the family, is very different from that of the H3BP P4QSO$_4$ family. Not only that, but while the H3BP family starts from a steady orbit, the family in the Jupiter–Europa CR3BP model starts from a swing QSO with a very important symmetric swing motion. For this reason, when comparing Figures 5.24c and 5.24d, where the UA and DA branches of the H3BP family are depicted, respectively, with Figures 6.15c and 6.15c, where the CR3BP family is shown, the shape is clearly different. Hence, the family studied in here is composed by orbits in which the swing motion is transforming. At the beginning of the family this motion is the one that characterized the symmetric families with an x-axis swing. As the family is continued, this motion evolves towards a more vertical swing. Nonetheless, the pure vertical swing that characterized the asymmetric families in the H3BP is never reached, as even at the end of the family the influence of the RSS QSO from which this family emanates is very noticeable in the shape of the orbits.

Let now analyze the evolution of the characteristics of the family and the way it compares with the symmetric P4QSO$_2$ family. Like it happened in the previous cases, right after the tangent bifurcation the energy of that branch of the symmetric family and the asymmetric family is almost the same. These two lines (Figure 6.15a) diverge some as the families are continued, but never reaching a big gap. Like in the high-energy cases, the asymmetric family is the one possessing a bigger energy. The case of the $|\rho|_{max}$ quantity, which is the other quantity showed in the figure, is a bit different. Unlike the previous cases, the values of this quantity diverge for the LSS symmetric branch and the asymmetric family since the first moment. Not only that, but also this time the asymmetric family is the one having the lowest values. The last part of the figure that needs to be analyzed is Figure 6.15b. The stability indices evolution of the asymmetric family is similar to that of the H3BP P4QSO$_4$ family. This means that the family is stable for the out-of-plane motion but unstable for the in-plane one, which is again a different behavior than the high-energy asymmetric families. Finally, due to the differences on the stability behavior of both the symmetric and the asymmetric families, the tangent bifurcation is in this case a subcritical pitchfork.

The next case is the one of multiplicity 6 whose symmetric family is the P6QSO$_2$ family depicted in Figure 6.16. This family shares a lot of characteristics with the P4QSO$_2$ family, but has one important difference with huge consequences. Unlike the rest of single-symmetric families for the Jupiter–Europa CR3BP, no tangent bifurcation is found for this family. Looking at Figure 6.16, it can be observed how for the in-plane motion each branch has a different behavior, one is stable and the other unstable, but with both staying close to a value of 2. More concretely, the LSS branch is unstable, while the RSS branch remains stable. This behavior is similar to the one observed for the P4QSO$_2$ family. However, at one point for the P4QSO$_2$ family, the unstable LSS branch becomes stable, but that never happens for this family. Like it was said before, in this section the families are continued until a collision with the secondary is approached, since the continuation method cannot move further past this

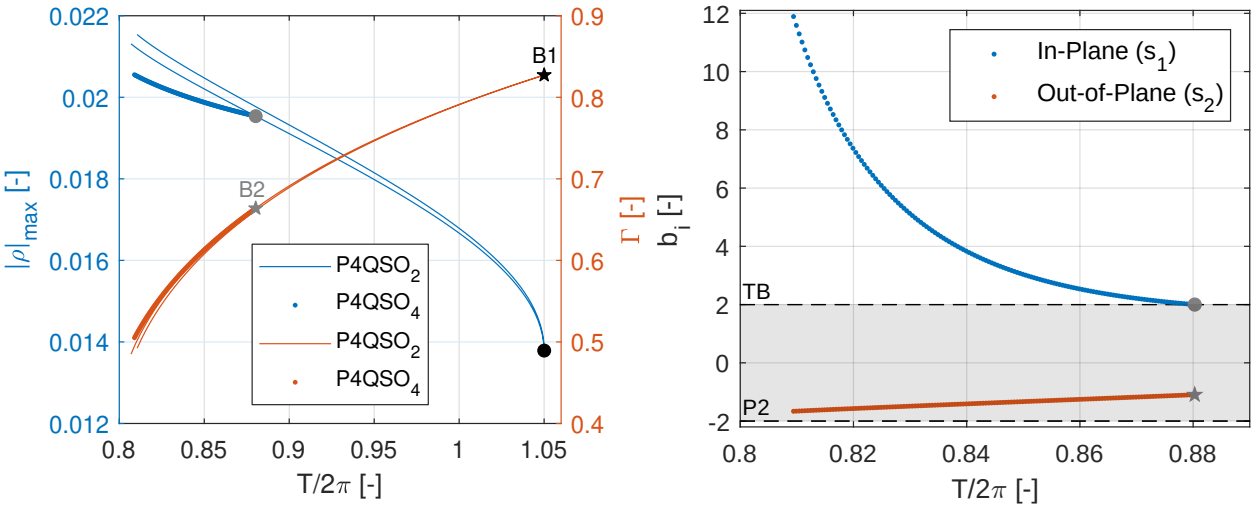

(a) Initial position and energy evolution tree

(b) Stability evolution

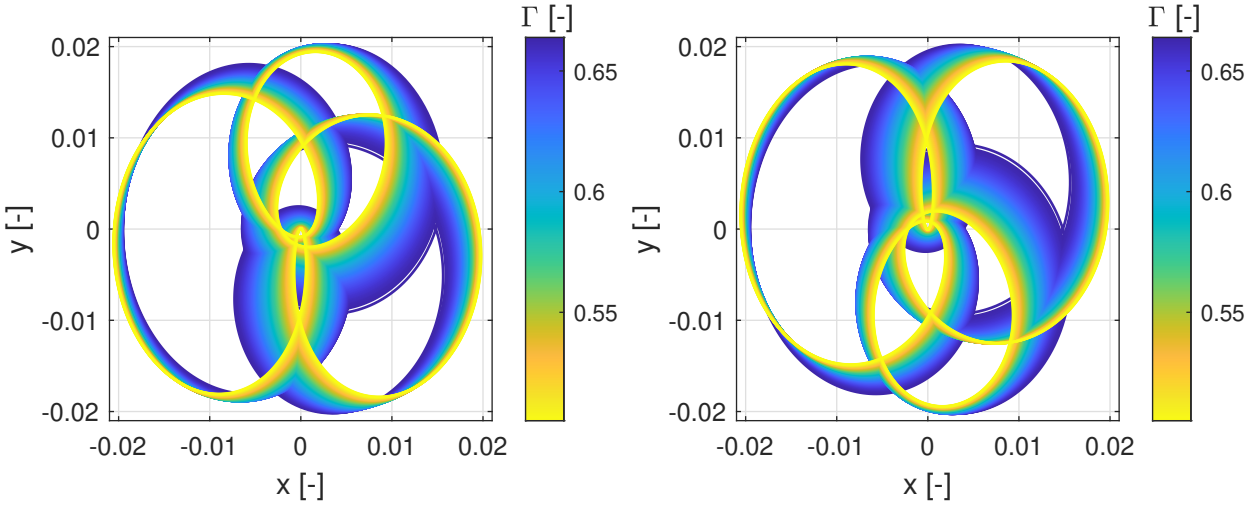

(c) UA branch

(d) DA branch

Figure 6.15: Low-energy asymmetric P4QSO$_4$ family in the Jupiter–Europa CR3BP

point. So, in this family, before that collision orbit is reached, the in-plane stability of the LSS branch is still unstable. In addition, not only the 'TB' line is not crossed in this branch, but also the stability index is monotonically increasing, starting from the 'B' orbit, for all the branch, moving farther from that line. One can think that, as the extension of the family achieved in the continuation until the collision point is short, maybe the tangent bifurcation does exist, but it is located after the collision. For this reason, two different strategies were implemented for trying to extend the continuation to orbits with both a retrograde and a prograde motion.

The first strategy was trying to move past the collision orbit with bigger sizes of the step. However, none of the step sizes tried and none of the continuation methods used during this strategy were able to achieve the desired orbits. The second strategy consisted on using some of the mixed orbits of the LSS branch of the H3BP P6QSO$_2$ family and trying to transition

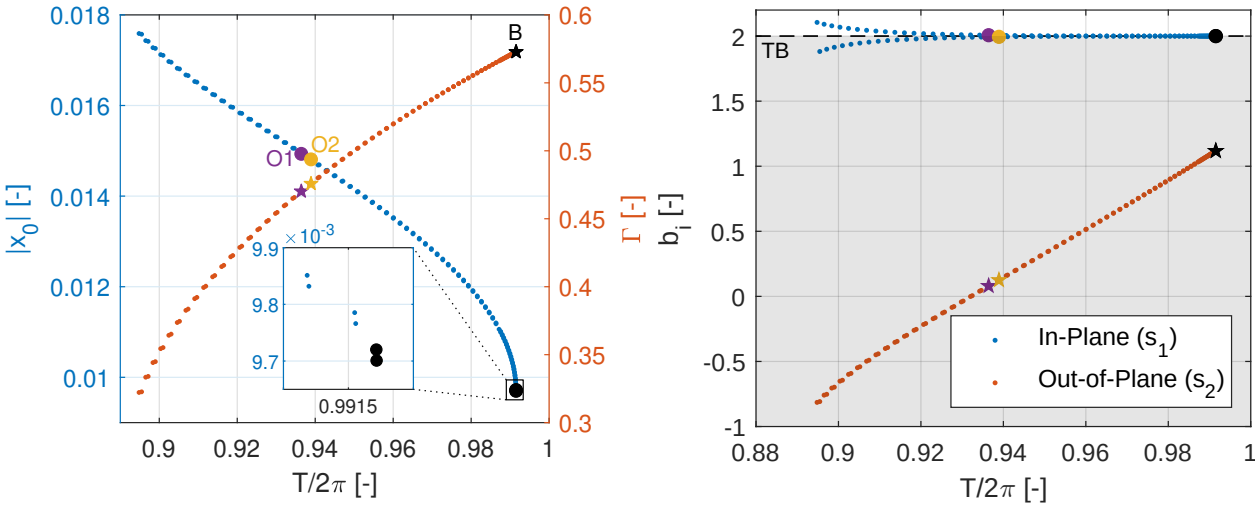

(a) Initial position and energy evolution

(b) Stability evolution

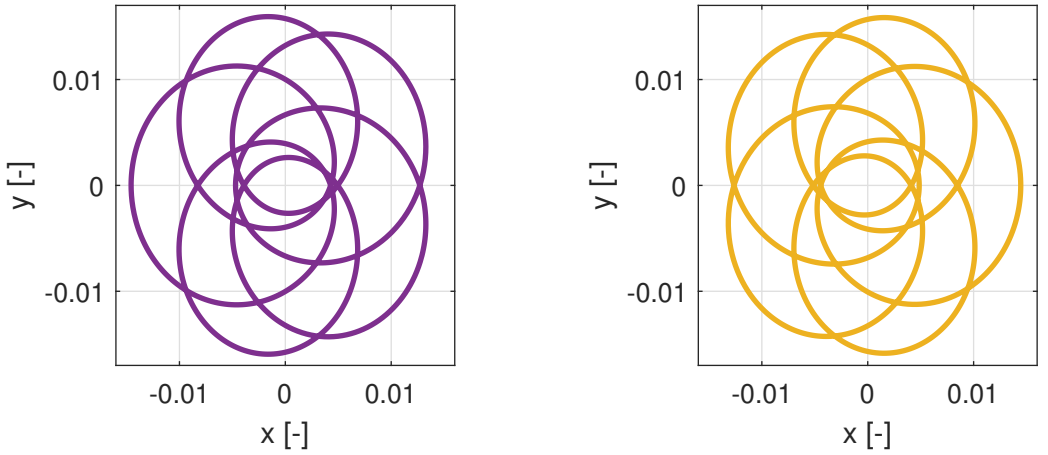

(c) Marked orbits

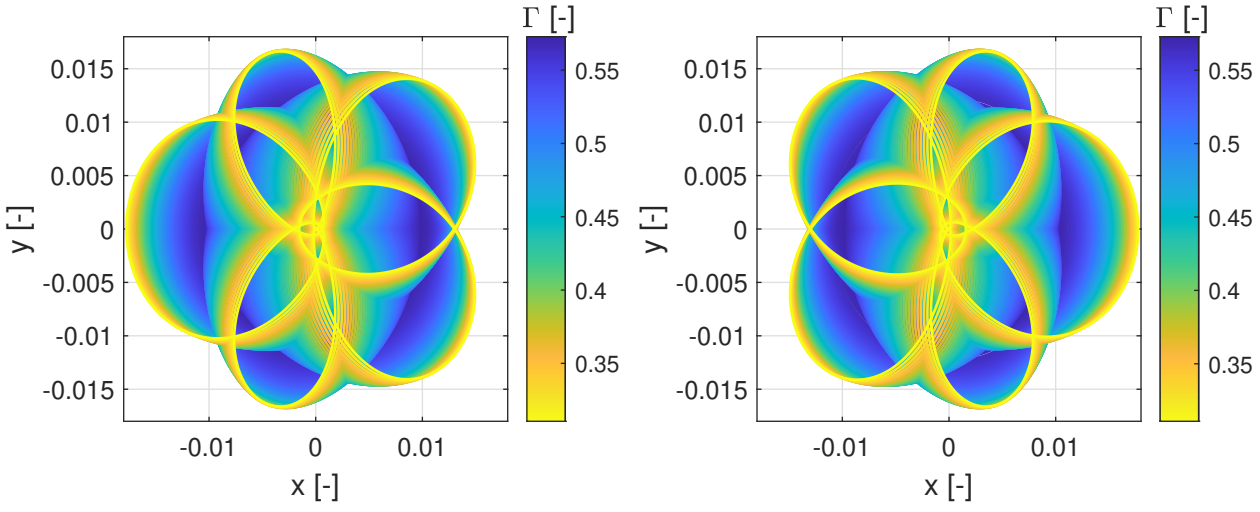

(d) LSS branch

(e) RSS branch

Figure 6.16: Low-energy P6QSO_2 family in the Jupiter–Europa CR3BP

them to the CR3BP. This transition from the H3BP to the CR3BP is, in general, done in one or two steps, depending on the orbit. For some orbits and when the μ value is small, the H3BP approximation is good enough so that the transition can be done directly in one step, transforming the H3BP coordinates directly to the desired μ-CR3BP model, and correcting to obtain the desired orbit. Nevertheless, most of the time the situation is not as ideal and the transition from the H3BP to the CR3BP can only be done for a smaller μ. After that, this orbit has to be continued in μ with a fixed period, using as many intermediate steps as needed until reaching the desired μ. For the case that is of interest in here, due to the complexity of the orbits involved, the two step approach was used. However, the transition to the Jupiter–Europa CR3BP model was not achieved for any of the orbits tried. Moreover, for most of the orbits, no CR3BP orbit was achieved even when using really small μ values, and for the orbits where this first step was successful, the continuation in μ failed for really small μ values. The reason behind this failure was always the proximity of the second primary, which became more prominent as the μ increased.

Even with the failure of both strategies to achieve mixed orbits, their non-existence cannot be confirmed. In order to be more certain of it, a regularization strategy should be implemented. Nonetheless, this is out of the scope of this investigation. Nevertheless, it does seem improbable that even if a part of a mixed branch existed this would lead to a tangent bifurcation that gave rise to an asymmetric family, as even for the H3BP the mixed branch was limited and taking into account the evolution that the in-plane stability index has for the computed part of the family. The situation takes place with the existence of the $P6QSO_4$ family of asymmetric orbits that did exist for the H3BP. Not only this family couldn't be found as a bifurcation from the $P6QSO_3$ family, but also when trying to transition a selection of the asymmetric orbits of the $P6QSO_4$ family from the H3BP to the CR3BP, that did not work either. Like what happened when trying to transition the symmetric orbits belonged to the $P6QSO_3$ family, the convergence could only be achieved for really small μ values. The reason behind that limitation on the μ values is that when the μ increases, again, the distance with the secondary is reduced too much, so the convergence fails.

Finally, there is an aspect of the $P6QSO_2$ family, outside of this lack of bifurcation, yet to be mentioned, that is the comparison between the two branches, LSS and RSS. The stability has already been commented, so let look at Figure 6.16a, where the energy and the initial position is shown. Like in all the single-symmetric families studied until now, excepting the $P7QSO_3$ family, the RSS branch is the one with the higher initial distance to the secondary. As for the energy, the LSS branch is the one with the highest values.

Taking into account that when trying to obtain the Jupiter–Europa asymmetric orbits of the multiplicity 6 from the H3BP ones, the only cases in which they could be closed were for very small μ values, one may think that maybe this family does not exist for Jupiter–Europa system, but it does exist for the other systems included in this work with a smaller μ. For that reason, the symmetric $P6QSO_2$ family is analyzed for the Mars–Phobos system, the one with the smallest μ out of the 4 systems included in this work. This family is shown in Figure 6.17 and, in general, is very similar to that of the Jupiter–Europa system. The first difference is that due to the smallest μ value, the differences between the two branches for the energy and the initial position are even smaller and cannot be appreciated in Figure 6.17a